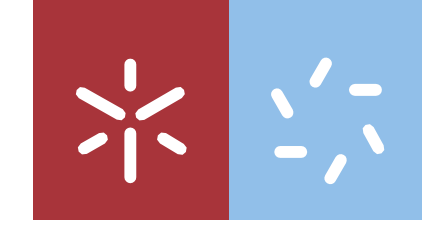Carlos Afonso Carvalho Pereira

Immunomodulation potential of *Cynara cardunculus* leaves extracts on *in vitro* skin models

January 2023

Immunomodulation potential of *Cynara cardunculus* leaves extracts on *in vitro* skin models

Carlos Pereira

UMinho | 2023

Universidade do Minho
Escola de Ciências

Carlos Afonso Carvalho Pereira

Immunomodulation potential of *Cynara cardunculus* leaves extracts on *in vitro* skin models

Tese de Mestrado

Mestrado em Biologia Molecular, Biotecnologia e

Bioempreendedorismo em Plantas

Trabalho efetuado sob a orientação da

Professora Doutora Andreia Gomes

E coorientação da

Doutora Teresa Silva Brás

Janeiro 2023

DIREITOS DE AUTOR E CONDIÇÕES DE UTILIZAÇÃO DO TRABALHO POR TERCEIROS

Este é um trabalho académico que pode ser utilizado por terceiros desde que respeitadas as regras e boas práticas internacionalmente aceites, no que concerne aos direitos de autor e direitos conexos.

Assim, o presente trabalho pode ser utilizado nos termos previstos na licença abaixo indicada.

Caso o utilizador necessite de permissão para poder fazer um uso do trabalho em condições não previstas no licenciamento indicado, deverá contactar o autor, através do RepositóriUM da Universidade do Minho.

ACKNOWLEDGMENTS / AGRADECIMENTOS

Consegui alcançar algo com que sempre sonhei: trabalhar num laboratório e adquirir o grau de Mestre. Desta vez levo no meu coração 5 anos e meio de experiências incríveis que vivi na Universidade do Minho. Tudo isto não era possível sem o apoio e carinho que recebi das pessoas que me foram acompanhando nesta etapa.

Em primeiro lugar quero expressar os meus maiores agradecimentos à professora Andreia Gomes, orientadora deste projeto, por me ter aceitado no seu laboratório e equipa de investigação, para realizar um projeto tão interessante. Agradeço o rigor e conhecimento científico que sempre demonstrou, a disponibilidade para tirar todas e quaisquer dúvidas e por tudo que me ensinou ao longo deste trabalho. Devo também um enorme agradecimento às Doutoras Fátima Duarte e Teresa Brás, por me terem orientado. Muito obrigado por, apesar da distância, a rápida resposta a qualquer dúvida e transmissão de conhecimento estar sempre a um clique de distância. Agradeço também pela facultação do extrato de cardo, importantíssimo para a realização deste projeto.

Quero agradecer também aos meus companheiros de laboratório, de salientar a Vanessa, o Mário e o Henrique, pela simpatia e se mostrarem sempre disponíveis para me ajudar. No entanto, devo o meu maior agradecimento, do fundo do meu coração, à Anabela, que desde o dia 1 me acompanhou (e aturou). Conseguiu suportar os meus esquecimentos, lentidão, confusões (etc.), mas mesmo assim esteve sempre lá para mim, sempre disponível para tirar qualquer dúvida, para me ensinar, e acompanhar com calma e simpatia. Obrigado por toda esta bagagem de experiência laboratorial que vou levar para a vida e vai ser essencial para a minha vida profissional!

Não posso deixar de agradecer à pessoa que mais tempo passou comigo nesta etapa, à Inês. Não podia ter melhor pessoa ao meu lado para partilhar orientadora com. Obrigado por todas as conversas, sorrisos, simpatia, amizade, almoços (especialmente aquele arroz de cenoura que tu fazes tão bem), apoio no laboratório e carinho. Não sei como teria sido este ano sem ti ao meu lado! Muito obrigado por tudo.

Agradeço também à minha família que me suportou durante este tempo todo. As boleias para o laboratório a horas absurdas, ouvirem-me a falar de assuntos como se eu estivesse a falar chinês, aturarem as minha mudanças de humor e cansaço, mas, principalmente, por todo amor e carinho incondicional que demonstraram e demonstram sempre. Fizeram de mim o Homem que sou hoje.

Por último (mas dos primeiros na minha vida), agradeço a todos os meus amigos, por todas as boas memórias e pelo apoio para nunca desistir! Muito obrigado a todos!

STATEMENT OF INTEGRITY

I hereby declare having conducted this academic work with integrity. I confirm that I have not used plagiarism or any form of undue use of information or falsification of results along the process leading to its elaboration.

I further declare that I have fully acknowledged the Code of Ethical Conduct of the University of Minho.

ABSTRACT

Nearly one-third of the world's population is affected by skin illnesses, which are the fourth most common cause of all human diseases. The high prevalence of skin conditions and the morbidity that comes with it over time, including extreme itching, constitute the burden of skin disorders. *Psoriasis vulgaris* is a common chronic inflammatory skin disease affecting up to 2–3% of the population worldwide. As there is no cure, therapies are often long-term and expensive, like biologics (for example, immunotherapy with antibodies). Some healthcare systems may be financially threatened by the high prevalence of skin problems and their related treatment costs. As the average life expectancy of the global population rises, these health issues are expected to be more prevalent.

Cynara cardunculus has been studied for the biological and pharmacological properties of the main sesquiterpene lactone present in its leaves, cynaropicrin. Among these, the anti-inflammatory potential effects of pure cynaropicrin and ethanolic extracts of *C. cardunculus* leaves (CLE) (submitted to membrane separation processes) in human skin cells, specifically HaCaT keratinocytes and BJ-5ta fibroblasts, were tested. In this work, a study of CLE activity in a co-culture of fibroblasts and keratinocytes was made, as these cells could be co-cultured to resemble the *in vivo* environment more nearly. Thus, with this model, we investigated the effects of CLE and cynaropicrin in a simulated inflammatory environment for the study of its effect on psoriasis.

The results revealed that both cell lines showed more sensitivity to cynaropicrin (IC_{50} of 2.11 µg/mL for BJ-5ta, and 3.72 µg/mL for HaCaT) than the extract (IC_{50} of 14.99 µg/mL for BJ-5ta, and 15.34 µg/mL for HaCaT). The optimization assays for the development of a co-culture model demonstrated that the Hoechst dye proved to be a good marker to get a proper visualization of the cells, and one that did not affect its proliferation, viability, and adherence. The exposure of the different co-culture models to LPS revealed that the proportion 1:1 (BJ-5ta:HaCat cells) may be more sensitive to LPS in terms of cell viability, implying the influence of keratinocyte cell quantity in the model. Better optimization of the co-culture protocol, and the screening for other cytokines that are closely related to psoriasis pathology, should be made in the future. Besides this, it would be interesting to stain both cells to get clear pictures of their interaction. The crosstalk between the cells could also be analyzed, with, for example, a trans-well migration assay.

Keywords: *Cynara cardunculus* leaves extracts, Cynaropicrin, Anti-inflammatory activity, Psoriasis, *In vitro* skin model

RESUMO

Quase um terço da população mundial é afetada por doenças de pele, que são a quarta causa mais comum de todas as doenças humanas. *Psoriasis vulgaris* é uma doença inflamatória crónica comum da pele que afeta 2-3% da população mundial. Como não há cura, as terapias costumam ser de longo prazo e caras, como é o caso dos biológicos (por exemplo, imunoterapia com anticorpos). Alguns sistemas de saúde podem ser afetados financeiramente pela alta prevalência de problemas de pele e o custo dos tratamentos associados. À medida que a esperança média de vida da população global aumenta, espera-se que esses problemas de saúde sejam cada vez mais prevalentes. *Cynara cardunculus* tem sido estudada quanto às propriedades biológicas e farmacológicas da principal lactona sesquiterpênica presente nas suas folhas, a cinaropicrina. Dentro destas propriedades, foram testados os potenciais efeitos anti-inflamatórios da cinaropicrina pura e extratos etanólicos de folhas de *C. cardunculus* (CLE) (submetidos a processos de separação por membrana) em células da pele humana, especificamente queratinócitos HaCaT e fibroblastos BJ-5ta. Neste trabalho, foi feito um estudo da atividade do CLE numa co-cultura de fibroblastos e queratinócitos, uma vez que estas células podem ser co-cultivadas para se assemelharem mais ao ambiente *in vivo*. Assim, com este modelo, investigamos os efeitos do CLE e da cinaropicrina num ambiente inflamatório simulado para o estudo do seu efeito na psoríase. Os resultados revelaram que ambas as linhagens celulares apresentaram maior sensibilidade à cinaropicrina (IC_{50} de 2.11 µg/mL nas BJ-5ta, e 3.72 µg/mL nas HaCaT) do que ao extrato (IC_{50} de 14.99 µg/mL nas BJ-5ta, e 15.34 µg/mL nas HaCaT). Os ensaios de otimização para o desenvolvimento de um modelo de co-cultura mostram que o corante Hoechst é um bom marcador para obter uma visualização adequada das células, que não afeta a sua proliferação, viabilidade e aderência. A exposição dos diferentes modelos de co-cultura ao LPS revelou que a proporção 1:1 (células BJ-5ta:HaCat) pode ser mais sensível ao LPS em termos de viabilidade celular, indicando uma influência da quantidade de células de queratinócitos no modelo. Uma melhor otimização do protocolo de co-cultura e a seleção de outras citocinas intimamente relacionadas à patologia da psoríase deve ser estudada no futuro. Além disso, seria interessante marcar ambas as células para obter imagens nítidas da sua interação. O *crosstalk* entre as células também poderá ser analisado, com, por exemplo, um ensaio de migração *trans-well*.

Palavras-chave: Extratos de folhas de *Cynara cardunculus*, Cinaropicrina, Atividade anti-inflamatória, Psoríase, modelos de pele *in vitro*

LIST OF CONTENTS

LIST OF FIGURES

LIST OF TABLES

LIST OF ABBREVIATIONS AND ACRONYMS

Cyn – Cynaropicrin

SL – Sesquiterpene lactones

CLE – *Cynara cardunculus* leaves extract

2D – Two-Dimensional

3D – Three-Dimensional

BSA – Bovine Serum Albumin

DAPI – 4',6-diamidino-2-phenylindole

DMEM – Dulbecco's Modified Eagle's high glucose Medium

DMSO – Dimethyl Sulfoxide

EDTA – Ethylene Diamine Tetra Acetic Acid

ELISA – Enzyme-Linked Immunosorbent Assay

FBS – Fetal Bovine Serum

PBS – Phosphate-Buffered Saline

IC$_{50}$ – Half Maximal Inhibitory Concentration

IL-6 – Interleukin-6

IL-18 – Interleukin-18

MTT – 3-(4,5-Dimethylthiazol-2-yl)-2,5-Diphenyltetrazolium Bromide

ELISA – Enzyme-linked Immunosorbent Assay

NF-κB – Nuclear Factor-κB

CHAPTER 1

Introduction

1. Introduction

Humanity's use of plants and plant products can be traced back to the beginning of human civilization. They provide man with all his needs in terms of shelter, clothing, food, and medicines (Saranraj *et al.*, 2016).

Of the wide range of benefits that plants and their compounds provide to humanity, one of the most important nowadays is their use as drugs to treat and prevent a wide range of human diseases. Their earliest use as medicine is documented back as far as 4000 years BC by the Sumerians, who used Opium, and by the Egyptians, who used plants like Aloe and Myrrha, dating from about 1550 BC (Sandberg & Corrigan, 2001). Chinese Traditional Medicine has also been around for at least 3000 years (Farnsworth & Soejarto, 2009). These examples show that plants yield many important drugs that humans may take advantage of, and more recently, with the advancements of biotechnology, were able to extract. Morphine, discovered in the early nineteenth century, paclitaxel, and artemisinin are drugs of a plant-based origin (Veeresham, 2012).

Plant-based medicines and botanical healthcare products are currently seeing a global upsurge in interest and use. For instance, the global herbal supplements market size grew from $10.14 billion in 2022 to $10.91 billion in 2023, and It is expected to grow to $14.79 billion in 2027 (Burslem, 2023).

The general public's growing interest in herbal remedies and products has boosted research interest in examining and comprehending the pharmacologically active components of medicinal plants (**Figure 1**) (Che & Zhang, 2019).
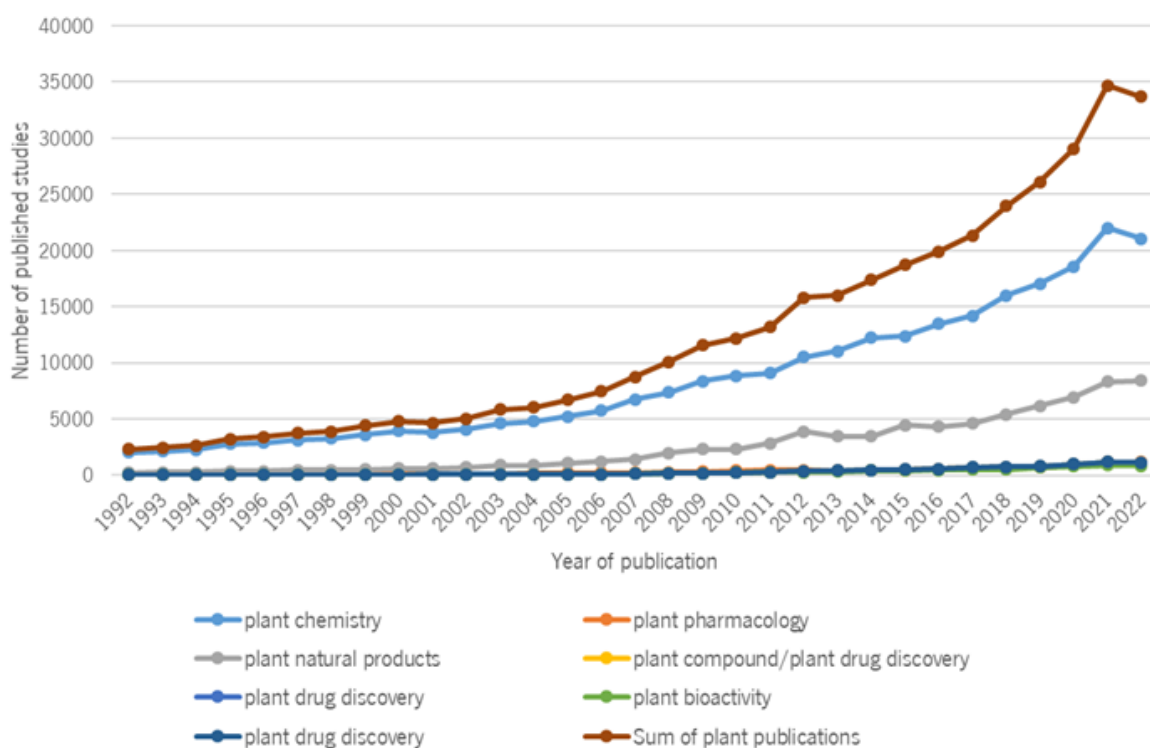
Figure 1 – Temporal evolution of plant-related publications. *Web of Science* trend analysis of plant-related publications throughout the years. It shows the huge increase in scientific interest in plant-derived natural products in pharmacology, chemistry, and drug discovery. In recent years, the number of publications with this tags has stabilized at over 30000 per year.

Approximately 80% of people worldwide rely on traditional medicines, most of which employ plant extracts for their primary healthcare. Higher plants' potential as a source of novel pharmaceuticals is yet largely unexplored. Only a small portion of the estimated 250 000–500 000 plant species has been studied in terms of their phytochemical composition (Saranraj *et al.*, 2016).

1.1. *Cynara cardunculus* L.

One plant whose extracts can potentially treat and prevent human diseases is *Cynara cardunculus* L. (from the Asteraceae family). In the last decade, *Cynara cardunculus's* potential as a source of bioactive compounds has been studied (Brás *et al.*, 2022; Paço *et al.*, 2022; Ramos *et al.*, 2013).

Commonly named 'cardoon', this perennial plant is a Mediterranean species that comprises three main varieties: *sylvestris* (Lam.) Fiori (wild cardoon), *scolymus* (L.) Fiori (artichoke), and *altilis* (DC.) (cultivated cardoon) (**Figure 2**). This specie, known for years to grow naturally in harsh conditions, typically in an arid climate with high temperatures and elevated salinity, is also known to have great biomass productivity (7,8 - 20,0 ton dry height/ha) under controlled cultivated conditions with adaptations against drought stress. It is used in the Mediterranean diet as an ingredient for soups and salads, and the flowers of *C. cardunculus* are traditionally used for making Iberian cheese, due to its proteolytic properties. Its leaves are particularly well known traditionally for their therapeutic potential as a diuretic, choleretic, cholagogue, antidiabetic, and antibacterial agent (Falleh *et al.*, 2008; Gominho *et al.*, 2018; Ramos *et al.*, 2017).

Ramos *et al.* (2013) analysed lipophilic extracts of *C. cardunculus* through gas chromatography–mass spectrometry. It were identified sesquiterpene lactones, namely cynaropicrin and deacylcynaropicrin, pentacyclic triterpenes (β- and α-amyrin, lupenyl and ψ-taraxasteryl acetates) and sterols (stigmasterol, 24-methylenecholesterol, campesterol, and Δ5-avenasterol). Besides this, it were found fatty acids, long-chain aliphatic alcohols and aromatic compounds. The two main lipophilic families of the identified chemicals were sesquiterpene lactones and pentacyclic triterpenes. The most prevalent sesquiterpene lactone was cynaropicrin, while the most prevalent pentacyclic triterpene was taraxasteryl acetate. Some of these molecules have therapeutic potential (Ramos *et al.*, 2013).
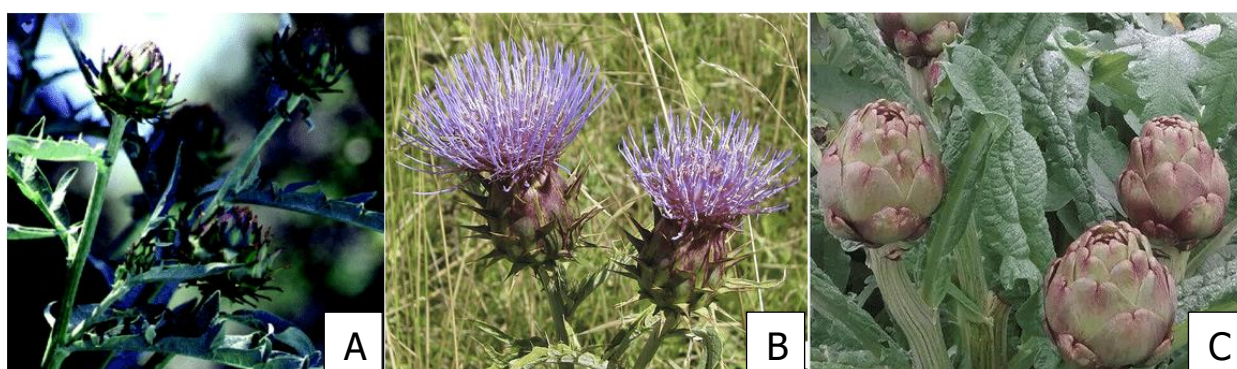
Figure 2 – *Cynara cardunculus* varieties. *C. cardunculus* var. *altilis* (A), *C. cardunculus* var. *sylvestris* (B) and *C. cardunculus* var. *scolymus*. Adapted from Gutiérrez D. *et al.*, 2020; Bermejo J. *et al.*, 2019.

Recently, the number of articles published about this plant has been rising and measures the scientific community's interest in this crop's properties (**Figure 3**) (Gominho *et al.*, 2018).
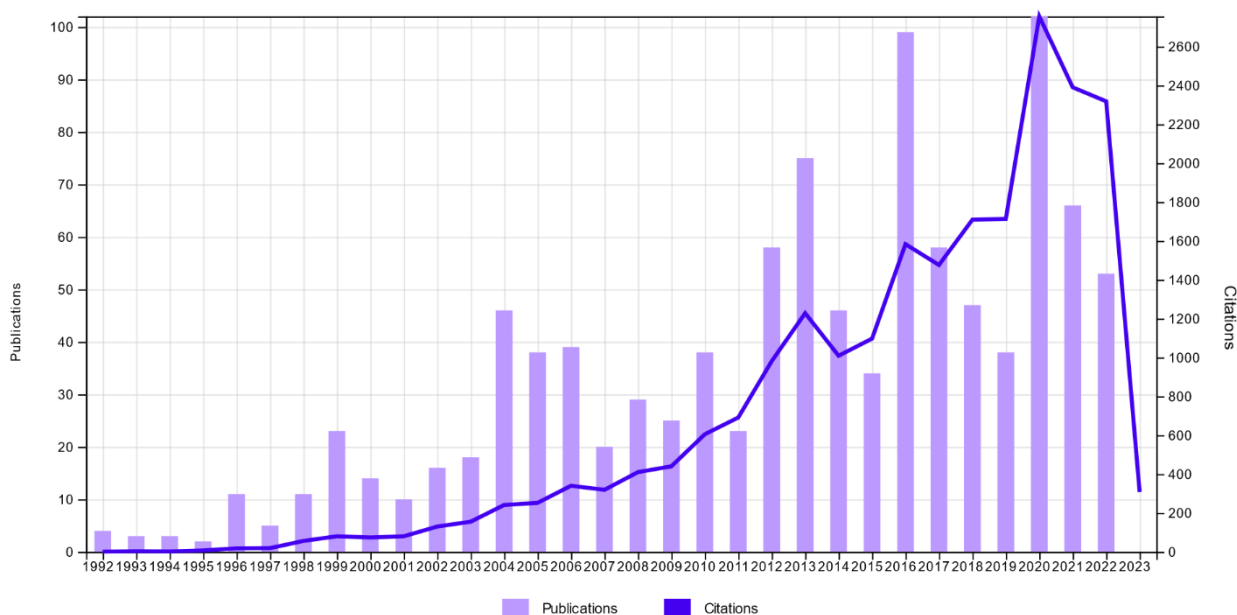
Figure 3 – Annual number of publications and number of citations in Web of Science searched for the topic "*Cynara cardunculus* L.", for the period 1992–2022. It shows a steady increase in publications, starting in 1998 and increasing rapidly after 2004. The number of citations and publications for this plant reached its peak in recent years.

1.2. Chemical and Extractives characterization of *C. cardunculus* L.

The health-promoting effects of *C. cardunculus* are associated with its rich secondary metabolites' composition (Falleh *et al.*, 2008). In contrast to primary metabolites, secondary metabolites are usually accumulated by plants in lesser amounts. Primary metabolites such as phytosterols, acyl lipids, nucleotides, amino acids, and organic acids are found in all plants and play vital and typically evident metabolic roles (Croteau *et al*, 2000). On the other hand, the number of secondary metabolites is impacted by both biotic and abiotic pressures, and its fluctuation is governed by genetic elements, plant development, and environmental factors. Cellular structures are thought to be protected by increased secondary metabolite synthesis in response to stressful conditions (Falleh *et al.*, 2008).

Sesquiterpene lactones (SL) are one of the major groups of plant secondary metabolites with a high biological potential, namely anti-inflammatory, highly abundant in Asteraceae plants, namely in *C. cardunculus* (Ghantous *et al.*, 2010; Ramos *et al.*, 2013). From over the 6000 varieties of SL, cynaropicrin

has raised high scientific interest, due to its biological activities such as the regulation of major adhesion molecules CD29 and CD98, its anti-inflammatory response, and anticancer potential against breast cancer, via *in vitro* and *in vivo* models (Cho *et al.*, 2004; Ramos *et al.*, 2017). The leaves of cultivated cardoon are an excellent source of sesquiterpene lactones, mainly represented by cynaropicrin, with concentrations ranging from 87.4 g/kg DW (**Figure 4**).
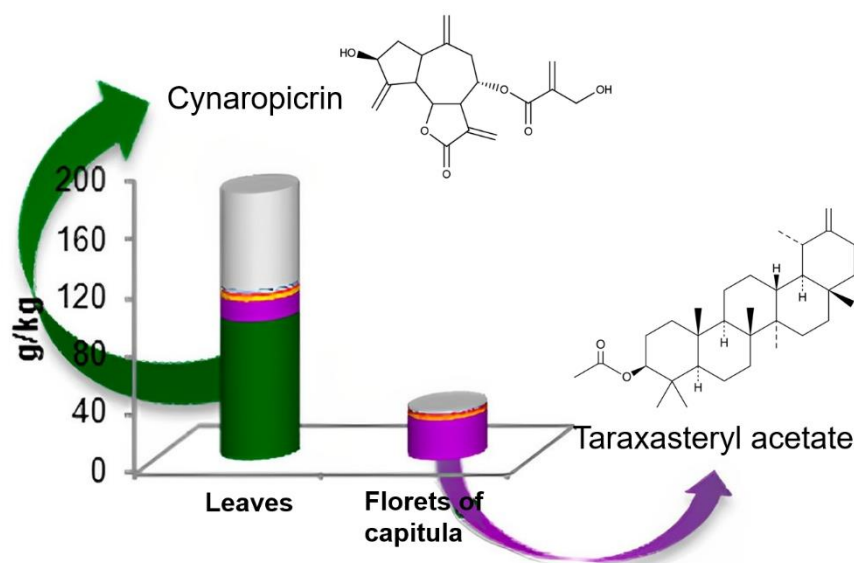
Figure 4 – Main compounds of *Cynara cardunculus* L. var. *altilis*. Cynaropicrin is the most abundant sesquiterpene lactone in the leaves, while taraxasteryl acetate is the main pentacyclic triterpene on the florets of capitula. Adapted from Ramos *et al.*, 2013.

Recently, Brás *et al.* described cynaropicrin extraction from *Cynara cardunculus* leaves and their optimization process using ethanol as solvent and pulsed ultrasound-assisted methodology, followed by fractionation by membrane separation processes to form a *C. cardunculus* leaves extract (CLE) (Brás *et al.*, 2020). This purification procedure is under a patent process (Bras T, Rosa D, Paulino AF, Neves LA, Crespo JG, Duarte MF. METHOD FOR OBTAINING CYNAROPICIN-RICH EXTRACTS, PPP 61514 INPI).

In that regard, chemical characterization studies of the extractives have shown the presence of lipophilic compounds, such as SL, pentacyclic triterpenes, fatty acids, sterols, long-chain aliphatic alcohols, aromatic compounds, among others in *C. cardunculus* (Ramos *et al.*, 2013).

Bioactive plant extracts have attracted a lot of attention in the context of transdermal medication administration and wound healing due to their biological characteristics, safety, and accessibility (Brás *et al.*, 2020).

1.3. Cynaropicrin

Cynaropicrin (**Figure 5**) is an SL, the most biologically significant class of secondary metabolites, of the guaianolide type. It is present in all morphological parts of *C. cardunculus* except in capitula florets, where the leaves showed the highest content of this compound, accounting for 87 g/kg dry weight (Ramos *et al.*, 2013). It has been established that cynaropicrin has a wide range of biological activities and exhibits extraordinary pharmacologic properties, including anti-hepatitis C virus, anti-parasitic, anti-tumor, anti-hyperlipidemic, antifeedant, antispasmodic, anti-photoaging agent, activation of bitter sensory receptors, suppression of NF-κB, and anti-inflammatory properties (**Figure 6**) (Elsebai *et al.*, 2016).
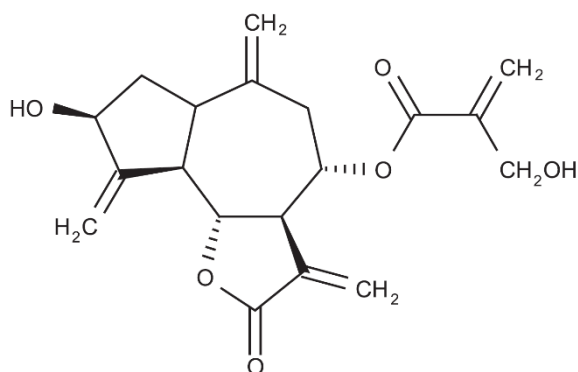
Figure 5 – Chemical structure of cynaropicrin ($C_{19}H_{22}O_6$). This molecule can form a homopolymer because of its 5-7-5 fused tricyclic skeleton and two hydroxyl groups on each side of its conformation. Cynaropicrin γ-butyrolactone ring is involved in most of the biological functions this molecule is known for. Obtained from Cho *et al.*, 2004.
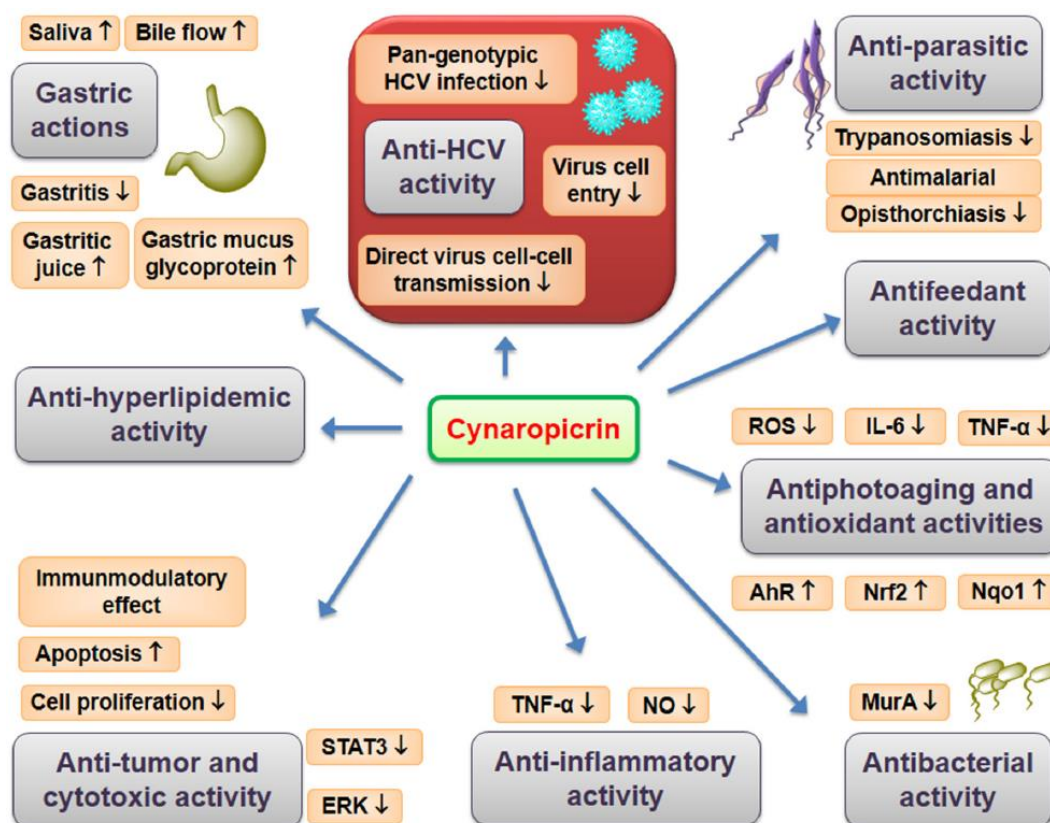
Figure 6 – Pharmacological effects of cynaropicrin. This sesquiterpene lactone has been associated with a wide range of health-promoting effects. For instance, cytokines like IL-6 and TNF-α, which play a major role in acute inflammatory reactions, are suppressed by cynaropicrin. Obtained from Elsebai *et al.*, 2016.

1.3.1. Anti-inflammatory activity of cynaropicrin

Inflammation is a biological response of the immune system to harmful stimuli, such as pathogens (viruses, bacteria), damaged cells, toxic compounds, and irradiation, to eliminate injurious stimuli and start the healing process. Thus, inflammation is a defense process that is essential for maintaining the organism's health and homeostasis (Chen *et al.*, 2018). These damaging stimuli initiate a chemical signaling cascade that activates specialized cells, like leukocytes, that produce and release several inflammatory cytokines, such as interleukin-1β (IL-1β), IL-6, and tumor necrosis factor-α (TNF-α). Besides cytokines, other pro-inflammatory mediators are produced and secreted, such as eicosanoids (prostaglandin E_2 and leukotriene B_4), reactive oxygen species (ROS), and nitrogen intermediates (like nitric oxide). The cytokines engage receptors and interact with them (IL-6R, TNFR-1, TNFR-2, TLR4, GM-

CSFR, etc.) (L. Kiss, 2022). The activation of numerous transcription factors is induced by the phosphorylation of several signaling molecules, including Janus kinase (Jak), nuclear factor kappa-B (NF-kB), and mitogen-activated protein kinase (MAPK). The level of inflammatory mediators in resident tissue cells is controlled by this coordinated activation of signaling molecules, which also attracts inflammatory cells from circulation (L. Kiss, 2022).

Cynaropicrin has been proven to have potent suppressive effects on TNF-α, a cytotoxin, and cytokine that causes inflammation and whose production is dysregulated in human conditions such as rheumatoid arthritis, psoriasis, and Alzheimer's disease (Cho *et al.*, 2000). This cytokine is also involved in tumorigenesis inhibition. Besides cynaropicrin's effects on TNF-α, it also suppresses cytokine-induced neutrophil chemoattractant-1 and nitric oxide release (Elsebai *et al.*, 2016).

This anti-inflammatory activity of cynaropicrin has been shown in several studies. Cynaropicrin (from *Saussurea lappa*) strongly inhibited the production of TNF-α from lipopolysaccharide-stimulated murine macrophage RAW264.7 cells, and U937 cells which are known producers of TNF-α. It also potently inhibited the release of nitric oxide from RAW264.7 cells, stimulated with lipopolysaccharide (LPS) and interferon-γ (INF-γ) (Cho *et al.*, 1998, 2000). Cynaropicrin inhibited the growth of splenocyte-derived lymphocytes and CTLL-2 cells that were activated by lipopolysaccharide, phytohemagglutinin, concanavalin A, and IL-2. All these inhibitory effects of cynaropicrin on TNF-α production were reversed by treatment with sulfhydryl compounds like L-cysteine and dithiothreitol, leading researchers to believe that cynaropicrin may contribute to the inflammatory response by preventing the production of inflammatory mediators and lymphocyte proliferation (Cho *et al.*, 2000). These findings suggest that cynaropicrin may be an effective treatment for both acute and long-term inflammatory disorders.

1.4. Psoriasis

Psoriasis is a chronic inflammatory cutaneous disease associated with the development of inflammatory plaques on the skin, mediated by the cells and molecules of both the innate and adaptive immune systems. It affects 2–3% of the population, with the most common clinical variant being *psoriasis vulgaris*, affecting approximately 85–90% of all psoriasis patients (Desmet *et al.*, 2017; Lowes *et al.*, 2014).

1.4.1. Pathogenesis and inflammatory mediators

The hallmark of psoriasis is sustained inflammation that leads to uncontrolled keratinocyte (KC) proliferation and dysfunctional differentiation (Ortiz-Lopez *et al.*, 2022). Pathogenesis of the disease is significantly influenced by the invasion of inflammatory immune cells. They interact with and activate KC, which causes the inflammatory cascade and disease development. Due to the high levels of interferon IFN-γ, TNF-α, and IL-12 as well as the presence of a significant number of CD4+Th1 and CD8+cytotoxic T cells type 1 (Tc1), psoriasis was once thought to be a Th1 cell-mediated disease (Rendon & Schäkel, 2019).

Additionally, the interaction of T cells with DCs results in the release of Th1-type cytokines, producing a "type 1" inflammatory environment. However, studies showed that Th17 cells that produce IL-17 as well as its effector molecules IL-17A, IL-17F, IL-22, IL-21, and TNF-α play an additional role in the pathogenesis of psoriasis (**Figure 7**). A third subset of Th cells has been implicated, namely the Th22 cells, due to their abundant secretion of IL-22 (Desmet *et al.*, 2017).
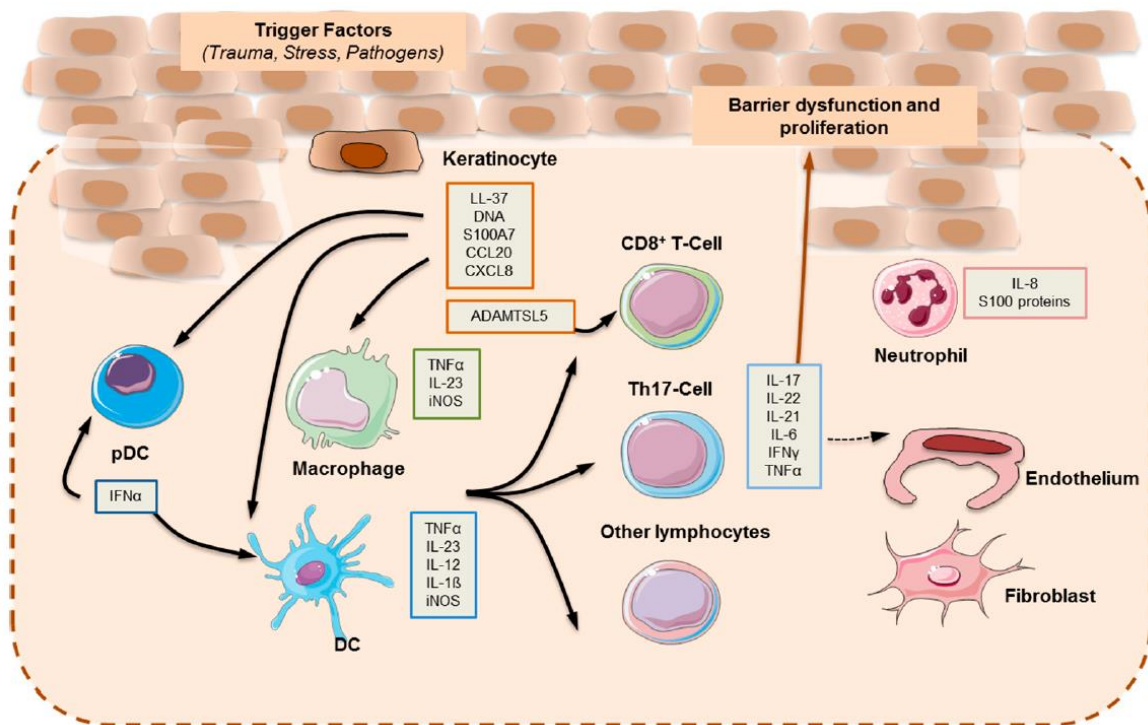
Figure 7 – The pathogenesis of psoriasis. Obtained from Desmet *et al.*, 2017.

1.4.2. Causes and triggers

Psoriasis has a complex pathophysiology, although genetics plays a major role, particularly in cases of plaque psoriasis with an early beginning (40 years). Heritability was estimated to be between 60 and 90 percent in twin, family-based, and extensive population-level investigations, which proved this. Genome-wide association studies have now found more than 60 susceptibility loci. Many of the probable causative genes are implicated in the NF-kappa B signaling system (TNIP1), type 1 interferon pathway (RNF113 and IFIH1), interleukin (IL)-23/Th17 axis (IL23R, IL12B, and TYK2), skin barrier function, and antigen presentation (HLA-C and ERAP1) (LCE3) (Raharja et al., 2021). This shows that the pathogenesis of psoriasis involves a complicated interaction between T cells, dendritic cells, and keratinocytes, with the IL-23/Th17 axis acting as the primary regulator of immune activation, chronic inflammation, and keratinocyte growth. Environmental factors like stress, obesity, beta-blockers, smoking, and lithium have been shown to make psoriasis worse. Pustular psoriasis appears to be genetically unique, with various susceptibility genes implicated, despite the relative lack of data (Raharja *et al*., 2021).

1.4.3. Current therapies

Psoriasis is a chronic relapsing disease, which often requires long-term treatment. Topical, photo, or systemic therapies are available for the treatment of psoriasis (Raharja *et al*., 2021). Glucocorticoids, vitamin D analogs, and UV therapy can all be applied topically to treat psoriasis in its early stages and less severe symptoms. Treatment options for systemic psoriasis are frequently needed. Comorbidities such as psoriasis arthritis are also very important when choosing a course of treatment. Modern targeted biological medications sometimes called small-molecule therapies are the product of a recent acceleration in the development of psoriasis treatments. Examples of these drugs are methotrexate, cyclosporin, and acitretin (Rendon & Schäkel, 2019). Another recent therapy are biologics, intricately manufactured molecules, such as monoclonal antibodies and receptor fusion proteins, which are used to treat psoriasis. The IL-23/Th17 axis and TNF-α signaling are two examples of particular inflammatory pathways that biologics target and are important in the development and chronic nature of the psoriatic plaque (Rendon & Schäkel, 2019).

The cynaropicrin and *C. cardunculus* extracts' previously described properties make them candidates for topical treatment that could potentially reduce psoriasis-related inflammation.

1.5. Skin histology

1.5.1. Skin cells: the role of fibroblasts and keratinocytes

The skin is the largest organ of the human body and acts as a barrier, protecting the internal organs and tissues, from the external environment (Wang & Li, 2020).

Fibroblasts are one of the most common cell types in the stroma, the area of a tissue or organ that plays a structural or connective role, as well as in the skin. It accomplishes a variety of duties and serves as the extracellular matrix's (ECM) structural underpinning during homeostasis for tissues and organs. Fibroblasts respond and transmit local signals under stress, can adapt to their surroundings, and change phenotypes, producing the components needed to replace damaged tissue in response to harm. In some diseases and pathological conditions, the extracellular matrix is produced in excess and collagen deposition is dysregulated, leading to irreversible organ malfunction or a disfiguring appearance (Dick *et al.*, 2022). During embryonic development, homeostasis, injury, healing, and remodeling, fibroblasts function as progenitors for specialized mesenchymal cell types, such as bone-forming osteoblasts or lipid-filled adipocytes, in addition to making connective tissue (**Figure 8**) (Plikus *et al.*, 2021).
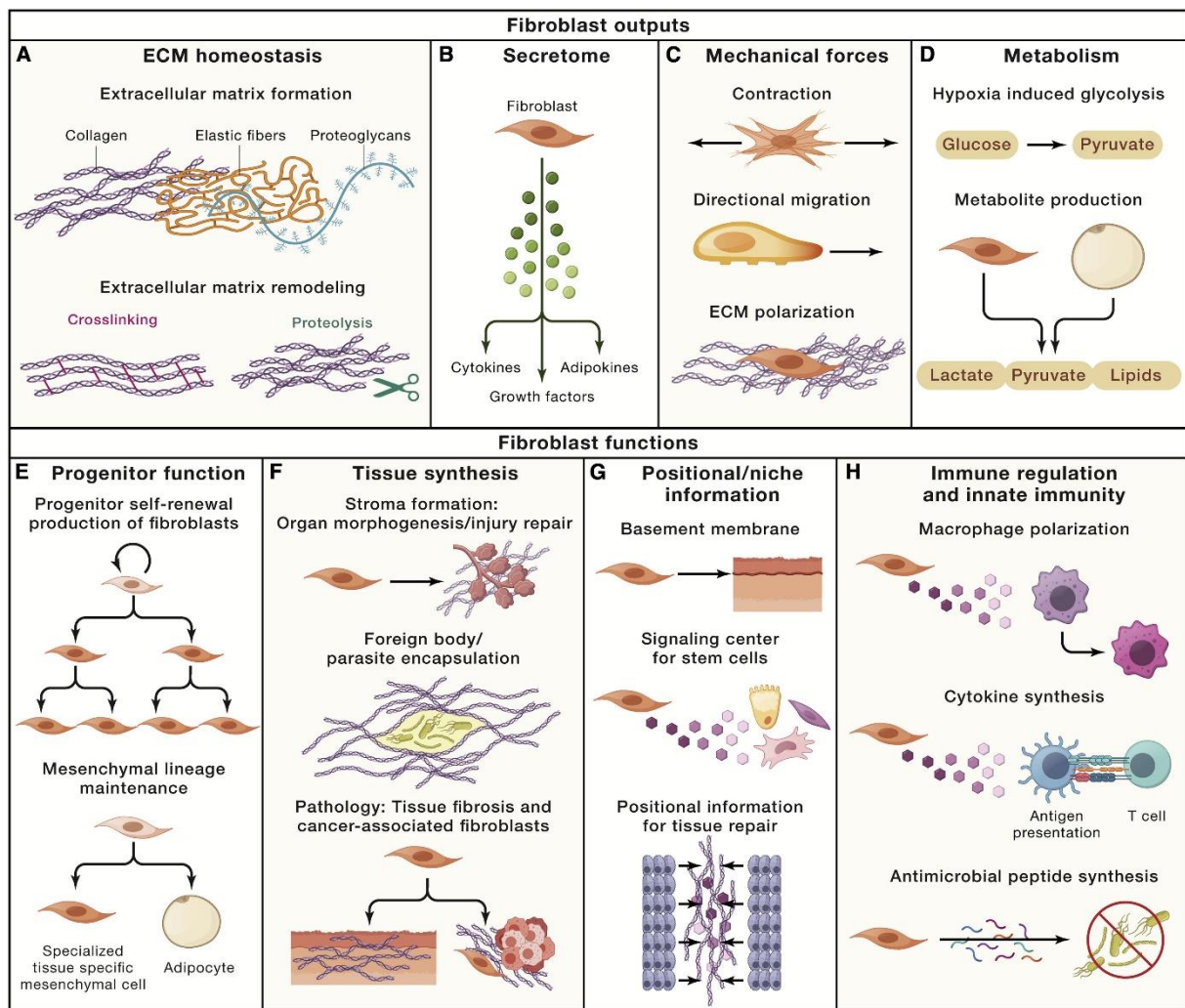
Figure 8 – Several outputs and functions of fibroblasts. Fibroblasts play a wide role of tasks in the human body, which include the secretion and remodeling of the ECM (A), secretion of signaling factors, like cytokines, to surrounding cells (B), mechanical force generation that confers to the organs and tissues some malleability and resistance to damage (C), regulation of tissue metabolism and production of metabolites (D); and some other functions like its role as a progenitor cell for mesenchymal lineages (E), its role in tissue synthesis during pathological or injury event (F), as sources of positional information (G), and as modulators of diverse innate and adaptive immune roles (H). Adapted from Plikus *et al.*, 2021.

Fibroblasts create inflammatory mediators in response to certain pathogens. There is proof that fibroblasts can produce key molecules involved in the innate immune response against pathogens, such as toll-like receptors (TLRs), antimicrobial peptides, proinflammatory cytokines, chemokines, and growth factors. TLRs (TLR-1 through TLR-10) can be expressed by fibroblasts to detect microbial substances or microbes. They can produce antimicrobial peptides including LL-37, defensins hBD-1, and, hBD-2, which have antibacterial properties. To trigger and attract inflammatory cells, they can also produce chemokines like CCL1, CCL2, CCL5, CXCL1, CXCL8, CXCL10, and CX3CL1, as well as the growth factors

granulocyte/macrophage colony-stimulating factor (GM-CSF) and granulocyte colony-stimulating factor (G-CSF). These also include proinflammatory cytokines like TNFα, INFγ, IL-6, IL-12p70, and IL-10 (Bautista-Hernández *et al.*, 2017).

TNF-α is a pro-inflammatory cytokine critical for host defense and clinically relevant to several barrier tissue chronic inflammatory diseases including psoriasis and inflammatory bowel disease. This is mainly due to its induction of IL-6 and CXCL8 in skin fibroblasts, and the expression of other proinflammatory cytokines and chemokines relevant to innate immunity (Cavagnero & Gallo, 2022).

Despite the enormous number of *in vitro* fibroblast research, the *in vivo* applicability of these cell culture data is still uncertain. Only recently has the full range of fibroblast traits and their lineage potential in the *in vivo* environment been thoroughly investigated (Plikus *et al.*, 2021).

Most of the epidermis, which is the outermost layer of skin and the first line of protection for the host, is composed of keratinocytes. Despite not being derived from bone marrow, keratinocytes have been shown to play a significant role in innate immune responses and activate adaptive immunity in the skin. Through a variety of receptors, named PRRs, keratinocytes detect certain microbial components and create effector molecules like pro-inflammatory cytokines (IL-1, IL-6, IL-18, TNF, and IFN), anti-inflammatory cytokines (IL-10), chemokines (IL-8, CXCL1, CXCL2, CXCL10, CCL2, and CCL20), to fend off infection. Additionally, these cytokines produced by keratinocytes can attract T cells and neutrophils, two types of immune cells, to the infection site taking part in the adaptive immune response. One example of this response is the enhancement of Th1 through the cytokine IL-18, part of the IL-1 family. IFN-γ and other cytokines produced by Th1 cells stimulate the activation of macrophages and other immune cells (Wang & Li, 2020).

In psoriasis, keratinocytes have a major role in the pathophysiology of the disease. During the initial phases of this disorder, keratinocytes produce trigger factors like LL37/nucleic acid complexes, lipid antigens, and so on, along with chemokines and cytokines from the IL-1 family and antimicrobial peptides (AMP) such β-defensins (HBD) and S100 proteins. The adaptive immune phase of the disease begins with high production of TNF-α by the dendritic cells and the consequent expansion of T lymphocytes, mainly Th17 and Th22, in an early stage of the disease, and, later, the type-1 interferon (IFN)-γ-producing T cells in the chronic phase. Keratinocytes impact the dendritic cells' immune functions by producing cytokines derived from the inflammasome pathway. A cytokine milieu, primarily made up of IFN-, TNF-, IL-17, and IL-22, is established by the T-cell infiltrate that is present during the late/chronic phase of psoriasis. This milieu directs the expression of specific and pathogenic gene signatures in keratinocytes, which causes them to overexpress several inflammatory mediators. The cytokines IL-22

and IL-17, in particular, cause keratinocytes to hyperproliferate and exhibit altered differentiative processes. Continuous interaction between keratinocytes and immune cells during the disease's amplification/chronicization phase promotes inflammation and hyperplasia (Albanesi *et al.*, 2018).
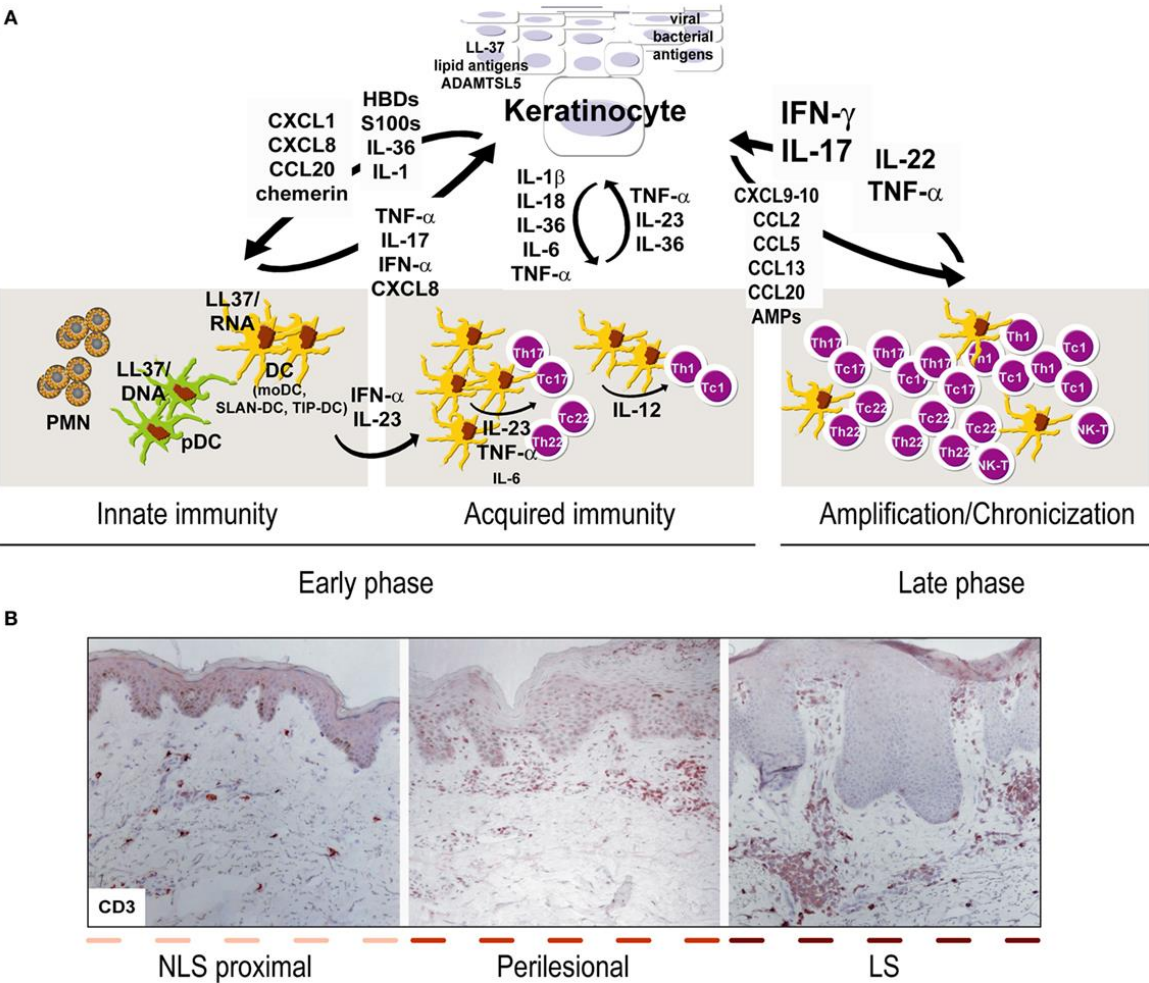
Figure 9 – Interaction between keratinocytes and immune cells in psoriasis. The development of the disease covers, in an early stage, innate immunity pathways, and the chronic phase starts with the involvement of acquired immunity pathways (A); The same psoriatic plaque, which includes lesional skin (LS), perilesional and non-lesional skin (NLS), can contain both early and late stages of the disease (with markers of CD3+T accumulation most prevalent in LS skin (B). Adapted from Albanesi *et al.*, 2018.

1.5.2. Monolayer *in vitro* models

Single-cell model

In monolayer models, only one cell type is considered at a time. As a result, in the case of psoriatic disease, keratinocytes or fibroblasts will be utilized to evaluate various situations or aspects of the disease, such as cell division or proliferation. With the aid of these models, a normal or a pathological cell type can be isolated to better understand its particular function (Jean & Pouliot, 2010).

The inability to reproduce results, loss of psoriasis-related gene expression, and growth issues make cultivating keratinocytes generated from psoriasis challenging. One way to counter this is via inducing psoriasis-associated features in human keratinocytes, by changing its culture medium. Desmet *et al.* (2017), managed to develop an *in vitro* psoriasis model where the disease phenotype was induced by the addition of a mix of pro-inflammatory cytokines, such as IL-1α, IL-17A, IL-6, and TNF-α. This model was a success in the evaluation of RNAi therapeutics. The advantages of a single-cell model are, then, its simple and highly reproducible methodology that allows fast screening of therapeutics (Desmet *et al.*, 2017). However, they prevent research on relationships between numerous cellular types, like the interactions between the dermis and the epidermis (**figure 10.A**) (Jean & Pouliot, 2010).

Co-culture model

Keratinocytes and fibroblasts could be co-cultured to resemble the *in vivo* environment more nearly. Using normal or involved (lesional) and uninvolved (non-lesional) psoriatic cells, several combinations have been assessed. It has been demonstrated that psoriatic fibroblasts cause the hyperproliferation of keratinocytes, but psoriatic keratinocyte continues to proliferate rapidly even when combined with normal fibroblasts (Desmet *et al.*, 2017).

A big advantage of co-cultures is that it allows the study of the precise functions of various cell types and their interaction with one another (**figure 10.A**) (Desmet *et al.*, 2017).

1.5.3. 3D skin equivalent models

Three-dimensional (3D) skin models are becoming more appealing for future therapeutic applications, such as in skin repair, tumor models, as well as the testing of medications and cosmetics. Separately cultivated cell types behave differently from those that are co-cultured. In recently created 3-D skin models, the "dermis" is composed of a layer of differentiated keratinocytes, while the "epidermis" is composed of fibroblasts that are "embedded" in the collagen matrix. A working basement membrane divides the epidermis from the dermis (Szymański *et al.*, 2020).

For some research questions, such as transdermal medication delivery tests, two-dimensional cell cultures are not appropriate since they do not mimic the typical structure of the skin. It would be better to use *ex vivo* human skin biopsies since they represent the interactions and mechanisms seen in complete skin. However, this approach is constrained by the availability and unpredictability of skin donors. As a result, bioengineered human skin substitutes have been created. These skin-like substitutes are made of extracellular matrix elements and primary human cells (fibroblasts, KC, and/or stem cells). These models offer a 3D microenvironment, making them preferable to monolayer models. Two different types of skin substitutes can be created as *in vitro* test systems: full-thickness skin equivalents, which have both an epidermal and dermal skin compartment, and epidermal equivalents, which only contain a multi-layered epidermis (**figure 10.B**) (Desmet *et al.*, 2017).
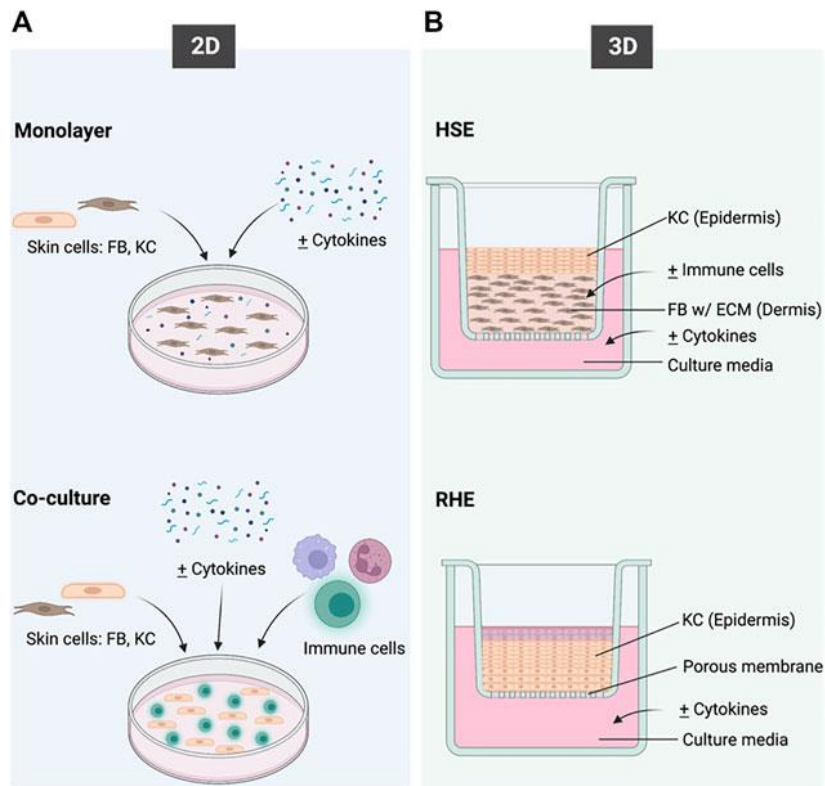
Figure 10 – Overview of *in vitro* 2D and 3D skin cell culture models. (A) Two-dimensional co-culture systems. Skin cells, cytokines, and small molecules can be mixed and cultured together in the same culture medium. (B) Three-dimensional skin equivalent: HSE is a bi-layered skin model (epidermis and dermis); and RHE is a model of a fully differentiated epidermis without a dermal compartment. These models have been used to study the effects of inflammatory skin diseases (Obtained from Desmet *et al.*, 2017)

1.6. Aims

Nearly one-third of the world's population is affected by skin illnesses, which are the fourth most common cause of all human diseases. Despite their widespread visibility, the burden of skin diseases is sometimes overlooked. The high prevalence of skin conditions and the morbidity that comes with it over time, including extreme itching, constitute the burden of skin disorders. Psoriasis is one of several chronic inflammatory skin conditions, and new therapies, like biologics (for example, immunotherapy with antibodies), can be expensive. Some healthcare systems may be financially threatened by the high prevalence of skin problems and their related treatment costs. As the average life expectancy of the global population rises, these health issues are expected to be more prevalent.

Cynara cardunculus have been extensively studied and the biological and pharmacological properties of the main sesquiterpene lactone present in the leaves, cynaropicrin, have been reported in several studies. Among these, the potential anti-inflammatory effects can be highlighted. From that, the anti-inflammatory potential of pure cynaropicrin and ethanolic extracts of *C. cardunculus* leaves (CLE) (submitted to membrane separation processes) in human skin cells, specifically HaCaT keratinocytes and BJ-5ta fibroblasts, were tested.

For that, we propose a study of CLE in a co-culture of fibroblasts and keratinocytes, as these cells could be co-cultured to resemble the *in vivo* environment more nearly than a monolayer. With this model, we intend to investigate the effects of CLE in a simulated inflammatory environment for the study of this extract on psoriasis.

CHAPTER 2

Materials and Methods

2. Materials and Methods

2.1. Reagents and equipment

The materials used in this work are listed in the table below.

Table 1 – Reagents and all equipment used in this work.

Reagent or Equipment	Company	Reference
Hygromycin B	BD Pharmigen	556547
Dulbecco's Modified Eagle's Medium (DMEM)	Sigma-Aldrich	1001417958
Antimycotic/antibiotic mix	Sigma-Aldrich	A5955
Medium 199	Merck	T061-01
Fetal Bovine Serum (FBS)	Sigma	A7030
L-Glutamine	Sigma-Aldrich	3274
Hoechst 33342	Thermo Fisher	62249
Neutral Red	Sigma-Aldrich	50040
Sulfuric acid (H_2SO_4)	-	-
Dimethyl sulfoxide (DMSO)	Sigma-Aldrich	101719820
Ethanol (EtOH)	Carlo Erba	4146052
Sodium hydroxide (NaOH)	Sigma-Aldrich	S5881
Hydrochloric acid (HCl)	Sigma-Aldrich	H1758
Trypsin EDTA solution	Biochrom	L2103
Piroxicam	Sigma-Aldrich	1001237700
Cynaropicrin ($C_{19}H_{22}O_6$)	Cayman Chemical Company	25099
3-(4,5-Dimethylthiazol-2-yl)-2,5-Diphenyltetrazolium Bromide	Sigma	M2128
Trypan Blue	Sigma-Aldrich	T8154
Tween 20	Sigma-Aldrich	T8787

ELISA Human IL-6 (HRP)	Mabtech	3460-1H-6
Human Total IL-18 DuoSet ELISA	R&D Systems	DY318-05
Microplate reader SpectraMax Plus	Molecular Devices	-
Incubator Sanyo Electric Co.	Sanyo Electric Co.	-
Centrifuge 2-16k	Sigma	-
IX71 Inverted Fluorescent Microscope	Olympus	-

2.2. *Cynara cardunculus* L. extracts

Ethanolic leaves extracts of *C. cardunculus* were obtained, as previously described, by pulsed ultrasonic-assisted extraction (PUAE) (Brás *et al.*, 2019) (patent - WO2017203498 Processes for extracting cynaropicrin from leaves of *Cynara Cardunculus* L.), and further fractionated by membrane separation to obtain a cynaropicrin *C. cardunculus* leaves rich extract.

In this work, pure cynaropicrin and extract of *C. cardunculus* leaves obtained by PUAE followed by membrane fractionation process (**Table 2**), were tested. This extract was kindly provided by Doctor Fátima Duarte, from the Bioactive Research Group from CEBAL.

Table 2 - *Cynara cardunculus* leaves extract characterization. It is obtained by PUAE followed by a membrane fractionation process. Cynaropicrin is the main compound of the extract.

Sesquiterpene lactone	mg/g extract
Cynaropicrin	376.20
Aguerin B	5.86
Grosheimin	9.03
11,13-dihydroxy-8-deoxygrosheimin	313.15
Cynaratriol	2.38
Deacylcynaropicrin	7.19
11,13-dihydro-deacylcynaropicrin	0.16
Total SL (%)	**71.4**

2.3. Cell lines and culture conditions

This study used two cell lines: BJ-5ta human fibroblast and HaCat human keratinocytes from ATCC (American Type Culture Collection) (**Figure 11**). BJ-5ta are hTERT-immortalized cells isolated from the foreskin of a male patient, usually used in toxicology research; while HaCaT are spontaneously immortalized aneuploid cells from adult human skin, widely used to study epidermal pathophysiology.

For the cell line BJ-5ta, cells were cultured in 4 parts of DMEM high glucose medium, containing 4 mM of L-glutamine and 1.5 g/L of sodium bicarbonate, and 1 part of Medium 199, supplemented with 10% of heat-inactivated fetal bovine serum (FBS), 1% antimycotic/antibiotic mix and 0.01 mg/ml hygromycin.

HaCaT cells were cultured in the culture media (DMEM - high glucose) supplemented with 10% of FBS and 1% antibiotic-antimycotic mix. The maintenance of cell culture in 25 cm^2 polystyrene culture flasks (T25 flasks) was achieved by subculturing cells when 80% confluence was reached, by treatment with 0,05% and 0.25% trypsin/EDTA solution for BJ-5ta and HaCaT cell line, respectively, followed by inactivation of the process with culture medium.

Both cell lines were cultured in a humidified 5% CO_2 incubator at 37 °C.

To safeguard both cell lines for future experiments, aliquots were cryopreserved in liquid nitrogen. After being trypsinized and neutralized with culture medium, the cells were centrifuged at 100 g for 5 min. The pellet was resuspended into the respective cryopreservation medium and the suspension was added to cryo tubes, which were stored in a Coolcell at - 80 °C. The cryotubes were frozen and then kept in liquid nitrogen.
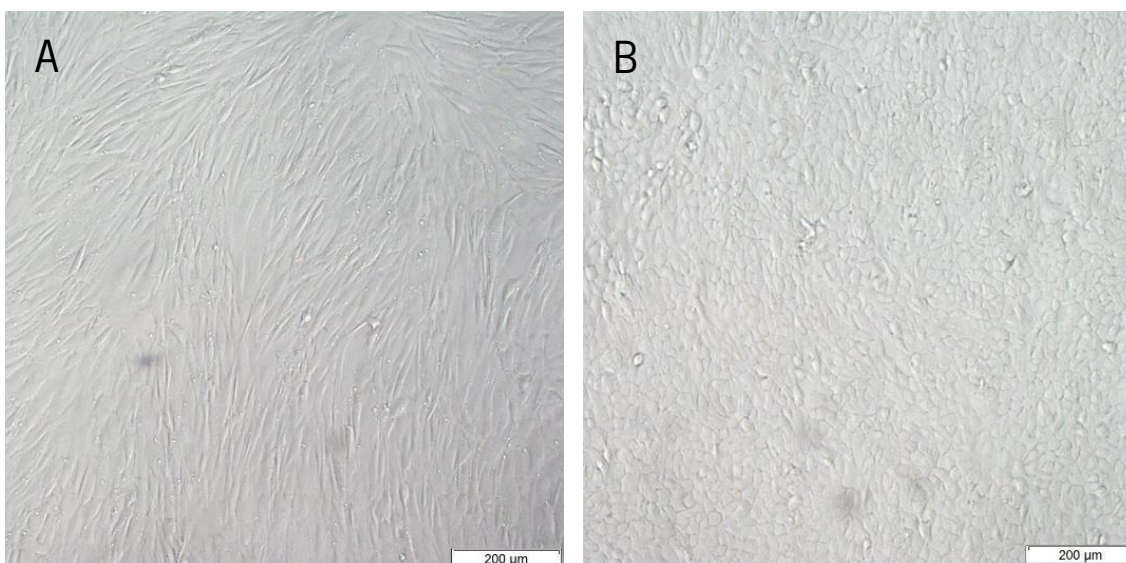
Figure 11 – Brightfield microscope images of fibroblasts BJ-5ta (A), and keratinocytes HaCaT (B), at a high confluency. Both cell lines are immortalized and of human origin, being extensively used in scientific research (images are at 100x magnification, scale bar 200 μm).

2.4. Optimization protocols for individual cell type visualization in co-cultures

2.4.1. Optimization of Hoechst concentration for vital staining

To evaluate the possibility of imaging the cells and the respective marker concentration to use, the Hoechst dye protocol was used. Hoechst (2'-[4-ethoxyphenyl]-5-[4-methyl-1-piperazinyl]-2,5'-bi-1H-benzimidazole trihydrochloride trihydrate) is a cell-permeable deoxyribonucleic acid (DNA) stain that displays blue fluorescence, at 460 to 490 nm, when excited by UV light. Adenine-thymine (A-T) sections of DNA are the preferred sites for Hoechst to bind. It is used for specifically staining the nuclei of living or fixed cells and tissues (Zhang & Kiechle, 1997).

Cells were plated at a density of 1×10^5 cells/mL for BJ-5ta cells, and 2×10^5 cells/mL for HaCaT cells, on 24-well tissue culture plates and left to adhere overnight at a 37 °C in a humidified CO_2 incubator. On the following day, both cell lines were exposed to concentrations of 2.5 μg/mL and 5 μg/mL of Hoechst dye, protected from light. After 10 min, the staining solution was removed, and the cells were washed 3 times with PBS 1x. A cell viability control was used, where the culture medium was replaced with the fresh medium (control without staining).

The cells were imaged immediately after the incubation with the dye, and 24, 48, and 72 h later, using a fluorescent microscope.

2.4.2. Evaluating the effect of the Hoechst staining on cell adherence and proliferation

To assess if the timing of dye incubation start had any influence on the proliferation, adherence, and viability of the cells, a BJ-5ta cell suspension was obtained at a density of $1x10^5$ BJ-5ta cells/mL or $2x10^5$ HaCaT cells/mL were used in the experiments. To evaluate the impact of the dye on the cells that weren't seeded yet, 1/3 of the total volume of each cell suspension was used. These cells were stained with 2.5 µg/mL of Hoechst dye for 10 min, protected from light, and were then centrifugated at 1 000 rpm for 5 min. The medium with the dye was removed and the resulting pellet was resuspended with the respective cell culture medium. The stained cells and the rest of the cells (the remaining 2/3 that didn't go through the staining process) were seeded on a 24-well tissue culture plate, separately, and left to adhere overnight at 37 °C in a humidified CO_2 incubator. On the following day, to evaluate the impact of the dye on the cells that were cultured overnight, the medium of the wells with the unstained cells was removed and these cells were incubated with a solution of 2.5 µg/mL Hoechst for 10 min, protected from light. The staining solution was removed, and the cells were washed 3 times with PBS 1x. After adding the respective culture medium, the cells from all the wells were imaged through visualization of the emitted fluorescent using an appropriate microscope, as described above. For this assay, a cell viability control was also used, where the culture medium was replaced with the fresh medium (control without staining for both cell lines).

After 24, 48, and 72 h, the same plates were visualized once again through a fluorescent microscope. On the last day of the protocol, an MTT assay was performed to evaluate cell viability. The results were normalized relative to the positive control (referred to as 100% cell viability) and expressed as percentages.

2.4.3. Optimizing Neutral Red dye staining concentration

To evaluate the possibility of additionally imaging HaCaT cells, the Neutral Red dye protocol was optimized. Neutral red ($C_{15}H_{17}ClN_4$) is a protonated diaminophenazine dye typically used in viability assessment as it is selectively absorbed by lysosomes and other acidic organelles in cells and can also

be used for supravital staining of living blood cells (Repetto *et al.*, 2008).

HaCaT cells were plated at a density of $2x10^5$ cells/mL, on a 24-well tissue culture plate and left to adhere overnight at 37 °C in a humidified CO_2 incubator. On the following day, the cells were exposed to concentrations of 15 µg/mL and 30 µg/mL of Neutral Red dye, for 2 h. The staining solution was then removed, the cells were washed with PBS 1x, and culture medium was added. A cell viability control was also used, where the culture medium was replaced with the fresh medium (control without staining).

After 24 and 48 h, the HaCaT cells were visualized in a fluorescent microscope.

2.4.4. Hoechst staining in co-culture models

To evaluate the ideal proportion between BJ-5ta and HaCaT cells in a co-culture disposition, and the correct staining of the BJ-5ta cells with the Hoechst dye in this setting, the following protocol was used: BJ-5ta cells were plated at a density of $1.18x10^5$ cells/mL ($5.9x10^4$ cells/well), on a 24-well tissue culture plate and left to adhere for 48 h at 37 °C in a humidified 5% CO_2 incubator. After the incubation period, the cells were stained with 2.5 µg/mL of Hoechst dye for 10 min, protected from light. The staining solution was then removed, the cells were washed 3 times with PBS 1x, and culture medium with HaCaT cells in different proportions was added, namely, $1.18x10^5$ cells/mL (1:1 BJ-5ta:HaCat cells), $2.36x10^5$ cells/mL (1:2 BJ-5ta:HaCat cells) and $3.54x10^5$ cells/mL (1:3 BJ-5ta:HaCat cells). The culture plate is left to adhere overnight in the same incubator conditions. In this assay, two controls were used: one where both cell lines were plated separately with and without staining, and a control with the different proportions of co-culture where the culture medium was replaced with the fresh medium (control without staining the co-culture).

After 24, 48, and 72 h, the plates were visualized with a fluorescent microscope, and pictures of the cells were taken.

2.5. Cell viability assessed by MTT assay

To assess cell viability and cytotoxicity of the CLE, the MTT test is employed to quantify cellular metabolic activity. This colorimetric assay relies on metabolically active cells converting the yellow tetrazolium salt 3-(4,5-dimethylthiazol-2-yl)-2,5-diphenyltetrazolium bromide (MTT) to purple formazan crystals through a reduction process. The MTT is converted to formazan by the NAD(P)H-dependent oxidoreductase enzymes found in the live cells. A solubilization solution is used to dissolve the insoluble formazan crystals, and a multi-well spectrophotometer is used to measure the absorbance at 570 nm of

the colored solution that results. The darker the solution, the greater the number of viable and metabolically active cells.

Cells were plated at a density of 1×10^5 cells/ml for BJ-5ta cells, and 2×10^5 cells/ml for HaCaT cells, on a 96-well tissue culture plate and left to adhere overnight at a 37 °C in a humidified CO_2 incubator. On the following day, cells were exposed to increasing concentrations of fractionated extract of *C. cardunculus* leaves (1, 10, 25, 50, 75, 100 µg/ml). Three controls were considered: one of cell death, where cells were incubated with a solution of culture medium with 30% DMSO ($^v/_v$); one of cell viability, where the culture medium was replaced with fresh medium; and a solvent control, where a percentage of ethanol present in the highest concentration of the tested extract was used. This last control is required since the extract is dissolved in ethanol.

In the following 24, 48, and 72 h of contact, cell metabolic activity was assessed by MTT viability assay. Briefly, the medium was removed from each well, and 100 µl of MTT reagent, prepared from 5 mg/ml stock solution and diluted with DMEM medium using a dilution factor of 1:10, was added. The cells were incubated again at 37 °C for 2 h. The MTT solution was then carefully aspirated, and the formazan crystals were dissolved in 120 µl of a DMSO/ethanol ($1:1(^v/_v)$) fresh solution. The absorbance of the samples was measured with a 96-well plate reader at 570 nm using a microplate reader. The results were normalized relative to the positive control (referred to as 100% cell viability) and expressed as percentages.

To calculate the half-maximal inhibitory concentration (IC_{50}) of the extract, the GraphPad Prism program was used.

2.5.1. Cell lines viability assessed by MTT assay in co-cultures

To study cell viability and later the expression of the pro-inflammatory cytokine IL-6 on the various proportions of co-cultured BJ-5ta and HaCaT cells, BJ-5ta cells were plated at a density of 1.18×10^5 cells/mL, on a 24-well tissue culture plate and left to adhere for 48 h at 37 °C in a humidified 5% CO_2 incubator. After the incubation period, the cells were washed 3 times with PBS 1x, and culture medium with HaCaT cells in different proportions was added: 1.18×10^5 cells/mL (1:1 BJ-5ta:HaCat cells), 2.36×10^5 cells/mL (1:2 BJ-5ta:HaCat cells) and 3.54×10^5 cells/mL (1:3 BJ-5ta:HaCat cells). The cells were, once again, left to adhere overnight. On the following day, the medium was discarded, and cells were stimulated with 5 µg/mL LPS for 8 h. Two controls were used: one where both cell lines were plated separately with and without LPS, and a control with the different proportions of co-culture where the

culture medium was replaced with the fresh medium (control without staining the co-culture). After incubation, the supernatants were removed, and fresh medium was added. 24 and 48 h later, the supernatant was collected and frozen at - 20 °C until a posterior evaluation of IL-6 expression, and an MTT viability assay was done. The results were normalized relative to the positive control (referred to as 100% cell viability) and expressed as percentages.

2.5.2. Evaluation of LPS-triggered inflammation by ELISA quantification of IL-6

To study the expression of the pro-inflammatory cytokine IL-6, BJ-5ta cells were seeded at a density of 1.8×10^5 cells/mL on a 12-well tissue culture plate and left to adhere overnight at 37 °C in a humidified CO_2 incubator. On the following day, the medium was discarded, and cells were stimulated with 5 µg/mL lipopolysaccharides (LPS) for 8 h. After stimulation, the culture medium was removed, and inflamed cells were exposed to two concentrations, 0.5 µg/mL and 1 µg/mL, of the extract and cynaropicrin for 12 and 24 h in the incubator. As a negative control, Piroxicam was used (at a concentration of 10 µg/ml), which is a commercial anti-inflammatory drug that inhibits the COX-2 enzyme isoform, responsible for the synthesis of prostaglandins that are mediators of inflammation, pain, and fever. The other two controls used were a positive control, where cells were incubated only with LPS added to the culture medium; and one of cell viability, where the culture medium was replaced with fresh medium.

After incubation, supernatants were collected and frozen at - 20 °C until testing. The quantitative determination of the pro-inflammatory cytokine IL-6 was performed with a Human IL-6 ELISA Kit according to the manufacturer's instructions. In this experimental procedure, a target-specific antibody coats the bottom of the wells of a microplate, and the plate is incubated overnight at 4 °C. The next day, the plate is washed with 1x Phosphate-Buffered Saline (PBS). After that, PBS with 0.05% Tween 20 containing 0.1% Bovine serum albumin (BSA) (incubation buffer) is added to block non-specific sites and the plate is incubated for 1 h at room temperature. The plates are washed with PBS + Tween 20 (0.05%), and the samples, standards, and controls are added to the wells and bound to the immobilized antibody (a process named capture,) and incubated for 2 h. Subsequently, the plates are washed again, and the sandwich is formed by the addition of the second antibody (known as a detector) that incubates for another hour. Then, the plates are washed, and an enzyme (Streptavidin-HRP) is added and incubated for 1 h. After that, a substrate solution, tetramethylbenzidine (TMB) is added and reacts with the target enzyme-antibody complex to produce a measurable signal (**figure 12**). After 10 min, the reaction was stopped with sulfuric acid (H_2SO_4). The optical density was measured at 450 nm using a 96-well

microplate reader. The concentration of IL-6 was determined through the substitution of the obtained values in the equation of the standard calibration curve calculated with default values of the target cytokine.
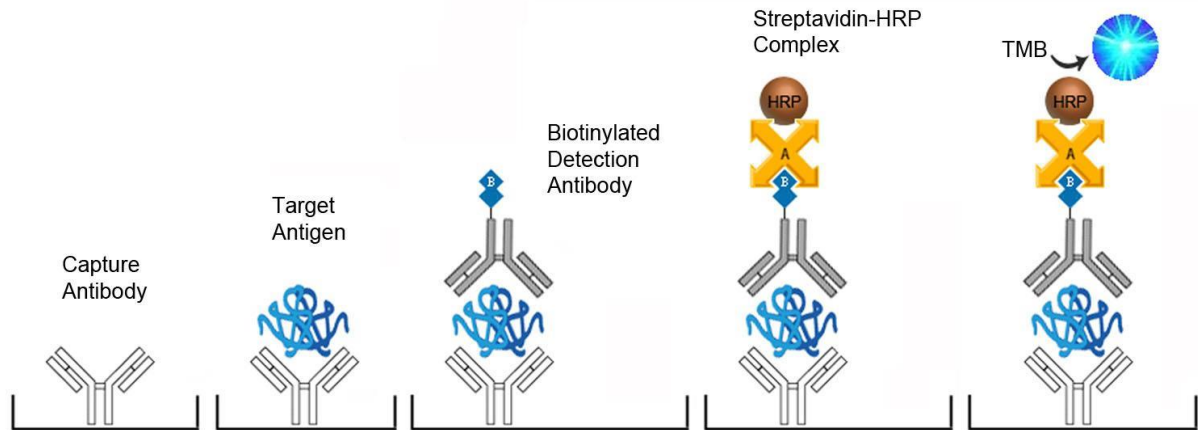

Figure 12 – Sandwich ELISA assay overview. The enzyme-linked immunosorbent assay (ELISA) used was for the quantitative detection of IL-6 in samples of cell culture supernatants. Obtained from *Isbio.*

2.5.3. ELISA quantification of IL-6 and IL-18 in co-cultures

To quantify and evaluate the effect of the LPS on the three co-culture proportions (1:1, 1:2, and 1:3 of BJ-5ta and HaCaT cells, respectively), the quantitative determination of the pro-inflammatory cytokines IL-6 and IL-18 was performed with a Human IL-6 ELISA Kit and a Human IL-18 ELISA Kit according to the manufacturer's instructions, as described earlier. The optical density was measured in a 96-well microplate reader, and the results were stated as the absolute value of IL concentration in the quantification of IL-6 and IL-18.

To analyze the effect of cynaropicrin and CLE on the three co-culture models described, after incubation with LPS, the culture medium was removed, and inflamed cells were exposed to three concentrations, 0.5 µg/mL, 1 µg/mL, and 5 µg/mL of the CLE extract and cynaropicrin for 12 and 24 h in the incubator. Piroxicam (an anti-inflammatory drug) was used as a negative control at a concentration of 10 µg/ml. As positive control, the cells were exposed to LPS without CLE or Cyn. The supernatants were collected and frozen at - 20 °C until a posterior evaluation of IL-6 and IL-18 expression. The optical density was measured in a 96-well microplate reader, and the results were then stated as the absolute values of IL-6 or IL-18 concentration.

2.6. Statistical analysis

All graphs and statistical analysis were performed using GraphPad Prism version 9.5.0 software (GraphPad Software, Inc., San Diego, CA, USA) and Microsoft Excel (2021). All data reflect results from multiple independent trials, carried out in triplicate. The standard error of the mean (SEM) was used to present continuous variables, while the number of categories was used to present categorical variables (as a percentage). To ascertain the differences between the means, two-way analysis of variance (ANOVA) and *post hoc* Tukey's and Sirdek's multiple comparison tests were utilized. Statistics were deemed to be significant at $p < 0.05$. In the figures, * denotes a p-value ≤ 0.05, ** a p-value ≤ 0.01, *** a p-value $\leq$ 0.001, and **** a p-value ≤ 0.0001.

CHAPTER 3

Results and Discussion

3. Results and Discussion

3.1. Extract and cynaropicrin effect on the cells

3.1.1. Cell viability assessed by MTT assay

Cell-based assays are frequently used to screen substances and analyze if the molecules that are being tested have an impact on cell growth or exhibit cytotoxic effects that ultimately result in cell death. As a result, several methods have been developed to accurately estimate how many viable cells are present at the end of the experiment (Riss *et al.*, 2016). One of the most used, for eukaryotic cells, is the MTT viability assay (Stockert *et al.*, 2018).

In the MTT tetrazolium reduction assay, viable active cells reduce the tetrazolium salt to a purple-colored formazan product via nicotinamide-adenine-dinucleotide (NAD(P)H) coenzyme and dehydrogenases within the mitochondria. The resultant insoluble and lipophilic product formed by the cleavage of its tetrazolium ring is impermeable to the cell membrane and so it accumulates in the metabolically active cells. The consequent intracellular purple formazan crystals can be solubilized and then quantified by absorbance at 570 nm using a plate reading spectrophotometer. The quantity of formazan is, presumably, directly proportional to the number of viable cells (Riss *et al.*, 2016; Stockert *et al.*, 2018).

To test the effect of the CLE on cell viability and toxicity and compare it to a previous work made with the same extract by Gonçalves A. (2020), an MTT viability assay was performed. As the CLE was obtained through fractionation by membrane separation processes, its content in cynaropicrin, the major compound of *C. cardunculus* extracts, was increased, and non-biologic interest compounds were removed. It was expected that the lowest concentrations of the CLE, obtained through this technique, were going to have a minimal impact on the viability of both BJ-5ta and HaCaT cell lines (Gonçalves, 2020). The results would also show the best range of concentrations of CLE to use for future assays without affecting cell viability.

All the results were normalized relative to the life control, which was considered as 100% of viability and represented by the line Y=100 in all the graphs. Absorbance values greater than the life control (>100%) indicate an increase in cell proliferation, while lower values suggest the inhibition of proliferation or cellular death. A decrease in cell viability greater than 30% was regarded as presenting a significant cytotoxic effect following ISO 10993-5:2009 guidelines for the biological evaluation of medical

devices.

Figure 13 shows the resultant data for BJ-5ta and HaCaT cell viability percentage in the function of increasing concentrations of the tested CLE. At 24 h, a significant reduction in cell viability has been already observed with the second lowest concentration (10 µg/mL), and a similar decrease was observed at the time points 48 and 72 h. Furthermore, the concentration of 1 µg/ml was the only one that did not exhibit significant toxicity after exposure to the CLE for 24, 48, and 72 h. These notions can be said for both cell lines.
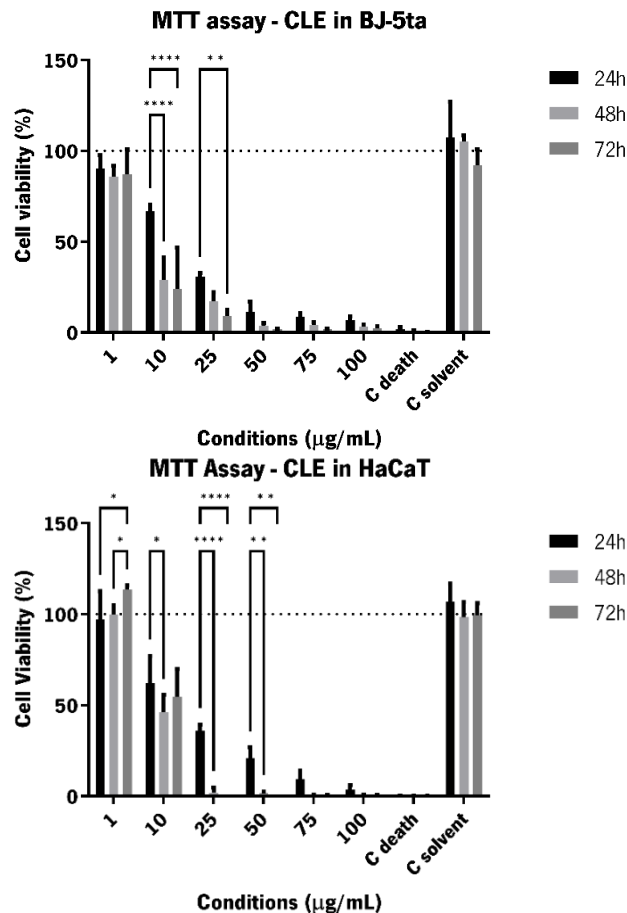

Figure 13 – Cell viability of fibroblasts BJ-5ta and keratinocytes HaCaT after exposure to CLE for 24, 48, and 72 h, evaluated by MTT assay. A reduction in cell viability is observed with concentrations equal or superior to 10 µg/mL. All the results were normalized relative to the life control, which was considered as 100% of viability and represented by the line Y=100. Analysed through a two-way ANOVA followed by Tukey's multiple

There is a clear toxicity of the extract with the increase in exposure time. In the case of BJ-5ta cells, we see that there are significant differences in cell viability between 24 and 48 h, as well as in 24 and 72 h for concentrations of 10 µg/mL, and between 24 and 72 h for a concentration of 25 µg/mL. With the HaCaT cells, there are more significant differences in cell viability, especially between 24 and 48 h, in the concentrations of 10, 25, and 50 µg/mL. These results can point to a more pronounced

effect of the CLE on cell viability in the period between 24 and 48 h.

The viability of BJ-5ta and HaCaT cell lines in function of increasing concentrations of pure cynaropicrin was also studied (**Figure 14**), with a range of concentrations based on previous works (Gonçalves, 2020). Through the analysis of these results, it is possible to conclude that the viability of the BJ-5ta cells decreases with lower concentrations of cynaropicrin when compared to the HaCaT cell line. For both cells, the concentration of 1 µg/mL did not depict considerable differences between incubation periods. However, there is a significant difference in cell viability between 24 and 72 h, as well as in 48 and 72 h for concentrations of 0.5 µg/mL, and between 24 and 72 h, along with 24 and 72 h for a concentration of 5 µg/mL, for the BJ-5ta cells. With the HaCaT cells, the only significant differences in cell viability were represented between 24 and 48 h as well as 24 and 72 h for a concentration of 5 µg/mL. Thus, these results can point to higher toxicity of the cynaropicrin with the increase in exposure time, especially in BJ-5ta cells, and a higher than 50% reduction in cell viability in concentrations of pure cynaropicrin above 5 µg/mL.
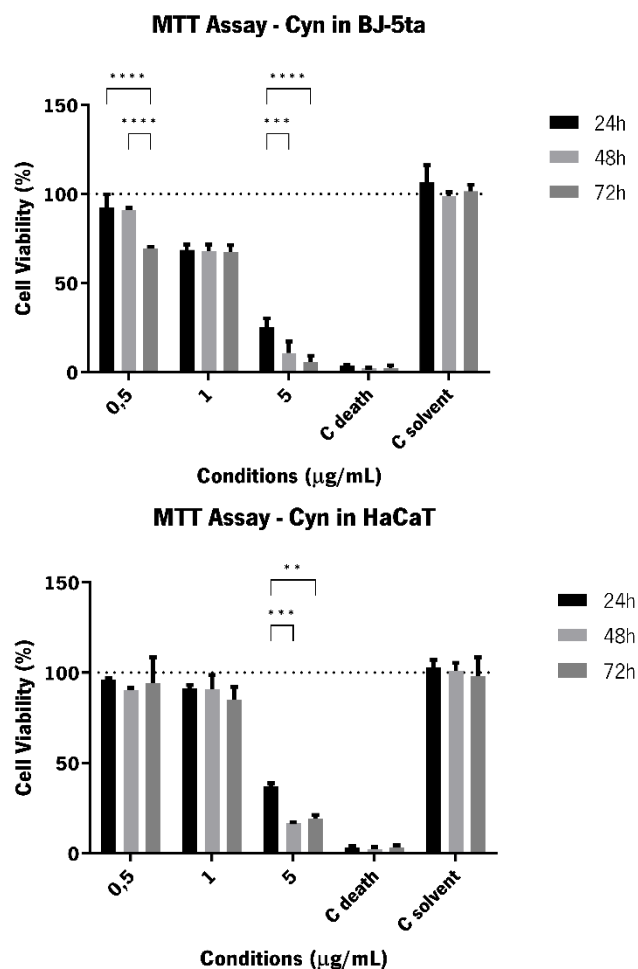

Figure 14 – Cell viability of fibroblasts BJ-5ta and keratinocytes HaCaT by MTT assay after exposure to pure cynaropicrin for 24, 48, and 72 h. Analyzed through a two-way ANOVA followed by Tukey's multiple comparisons test ($p < 0.05$; sample run in triplicates (n=3)).

3.1.2. IC_{50} of extracts and cynaropicrin

For drug discovery and pharmacology research, it is important to be able to precisely determine the inhibitor concentration required to inhibit a certain biological or metabolic activity. The IC_{50} is the concentration of an inhibitor where the response is reduced by half. In the case of compound testing on cells, inhibitory concentration curves, denoted IC_{50}, are dose-response curves that allow for determining the drug concentration required to reduce a population of viable cells by half when compared to the cells grown with no exposure to the drug or compound. The lower IC_{50}, the more potent the compound is in suppressing cell proliferation or causing cell death (Berrouet *et al.*, 2020).

Table 3 shows the IC_{50} values from CLE and pure cynaropicrin in both BJ-5ta and HaCaT cell lines, at three different incubation periods (24, 48, and 72 h). **Table 4** displays the IC_{50} values for the same conditions, obtained in previous work by Gonçalves A (2020). Through an HPLC characterization of the CLE, it was inferred that the percentage of cynaropicrin on the CLE was about 25% since there was a concentration of 5 mg/mL of cynaropicrin in the extract.

In the literature, it is reported that the IC_{50} of pure cynaropicrin is 6.19 ± 0.57 µg/mL, and the IC_{50} of the leaves lipophilic extract is 10.39 ± 0.57 µg/mL, for MDA-MB-231 cells (a breast cancer cell line) after an incubation period of 48 h (Ramos *et al.*, 2017). Compared to those results, the IC_{50} of the CLE in the BJ-5ta cell line is significantly lower, exhibiting higher toxicity than expected. However, this is not the case for the HaCaT cell line, where the value of IC_{50} is similar to the aforementioned results, within the same range of concentrations. Compared to the studies made in the same cell types by Gonçalves, A. (2020), the value of IC_{50} for the BJ-5ta cell line at the periods of 24, 48, and 72 h, is also lower. With the HaCaT cells, however, only the IC_{50} after 24 h displays a decreased value.

Regarding cynaropicrin, the results show higher cytotoxicity (a lower IC_{50}) in both cell lines and all incubation periods, when compared to the extract. Although the CLE concentration in cynaropicrin was increased due to the extract being subjected to membrane fractionation, it was anticipated a higher value for the IC_{50} of the CLE than that of pure cynaropicrin. This is due to plant extracts being normally more diluted than the pure compounds isolated from them and the fact that synergistic and antagonistic interactions between compounds can decrease their toxicity and lead to healthy beneficial interactions (Vaou *et al.*, 2022). The IC_{50} values of cynaropicrin were also more cytotoxic to BJ-5ta and HaCaT cells when compared with IC_{50} values from **Table 4**. However, the findings support the notion that the BJ-5ta cell line is more sensitive to cynaropicrin at increasing doses than HaCaT cells. This might be because keratinocytes, which serve as the skin's first line of defense against environmental stimuli, have adapted

to be more resilient to them (Wang & Li, 2020).

Table 3 – IC$_{50}$ values from fractioned CLE and pure cynaropicrin in BJ-5ta and HaCaT cell lines, at 24, 48, and 72 h. These values are theoretical and were calculated using the GraphPad Prism software.

		24 h	48 h	72 h
BJ-5ta	CLE	14.99 ± 0.94 μg/mL	4.78 ± 0.55 μg/mL	4.17 ± 0.82 μg/mL
	Cyn	2.11 ± 0.22 μg/mL	1,54 ± 0.09 μg/mL	1,26 ± 0.82 μg/mL
HaCaT	CLE	15.34 ± 1.70 μg/mL	9.62 ± 0.27 μg/mL	10.10 ± 0.98 μg/mL
	Cyn	3.72 ± 0.07 μg/mL	2.48 ± 0.24 μg/mL	2.41 ± 0.30 μg/mL

Table 4 – IC$_{50}$ values from cynaropicrin in BJ-54ta and HaCaT cell lines, at 24, 48, and 72 h. These values were obtained from Gonçalves A., 2020.

		24 h	48 h	72 h
BJ-5ta	CLE	21.38 ± 2.23 μg/mL	10.68 ± 1.88 μg/mL	6.42 ± 0.50 μg/mL
	Cyn	4.94 ± 0.51 μg/mL	2.78 ± 0.19 μg/mL	1.78 ± 0.57 μg/mL
HaCaT	CLE	21.45 ± 2.43 μg/mL	5.68 ± 1.26 μg/mL	2.18 ± 0.56 μg/mL
	Cyn	5.87 ± 1.50 μg/mL	1.38 ± 0.26 μg/mL	1.33 ± 0.10 μg/mL

3.1.3. Quantification of LPS-induced expression of IL-6 in fibroblasts

Immunological tests like the ELISA, are widely used in scientific research for their capacity to identify antibodies and antigens with only small amounts of test samples. This sandwich assay relies on the measure of the amount of the target cytokine that is bound between two layers of an antibody pair (capture and detection antibodies). A substrate solution is added to the sandwich complex to produce a measurable signal, represented by an observable color change. The signal intensity will be proportional to the concentration of IL-6 present in the samples (Paulie *et al.*, 2022). As a result, to measure the amount of pro-inflammatory IL-6, a Human IL-6 ELISA was performed.

IL-6 is a potent multifunction pro-inflammatory cytokine released by fibroblasts in response to

invading microorganisms or other cytokines. This interleukin and others, like IL-1 and IL-8, are responsible for conditioning the environment around sites of inflammatory lesions through the recruitment of immunological cells, such as macrophages and T cells, and induce angiogenesis (Kato-Kogoe *et al.*, 2010). Therefore, it plays an important role in the pathogenetic signaling pathway in diseases like psoriasis, where its enhanced expression increases keratinocyte growth and proliferation, and promotes epidermal hyperplasia (Saggini *et al.*, 2014).

To trigger the secretion of IL-6 by fibroblasts, LPS was used. LPS is a bacterial product present in almost all-negative bacteria and an extremely strong stimulator of innate immunity and inflammation processes (Alexander & Rietschel, 2001; Russell *et al.*, 2022).

The anti-inflammatory activity of the fractioned *C. cardunculus* extract and cynaropicrin on BJ-5ta fibroblasts stimulated with LPS was, therefore, measured through an IL-6 ELISA. The cells were incubated with LPS for a period of 8 h before being incubated with CLE and pure cynaropicrin for 12 and 24 h. Fibroblasts incubated only with LPS were used to test the inflammation without the presence of any other compounds, represented as the positive control. For the negative control, control of the anti-inflammatory effect, the cells were inflamed with LPS, and later added Piroxicam, a commercial anti-inflammatory drug. Fibroblasts without the supplement of any compounds were used to confirm that the cells exposed to the CLE and cynaropicrin would not display inflammation by themselves (life control). This control would also serve to evaluate the baseline levels of IL-6 in the cells. The concentrations of 0.5 and 1 μg/mL of cynaropicrin and CLE were chosen for this assay since they had little influence on the viability of BJ-5ta cells.

Figure 15 shows the concentration of IL-6 resulting from the inflammation of the BJ-5ta cell line with LPS and the respective anti-inflammatory activity of CLE and cynaropicrin. It was expected to see a reduction in the levels of IL-6 when the inflamed cells were exposed to both CLE and Cyn. However, when compared to the positive control, IL-6 levels weren't significantly lower, and even the negative control wasn't able to have strong anti-inflammatory activity.

However, between 12 and 24 h, there was a small decrease in IL-6 concentration in all of the conditions. This can potentially indicate more anti-inflammatory activity of the extracts and Cyn over time.
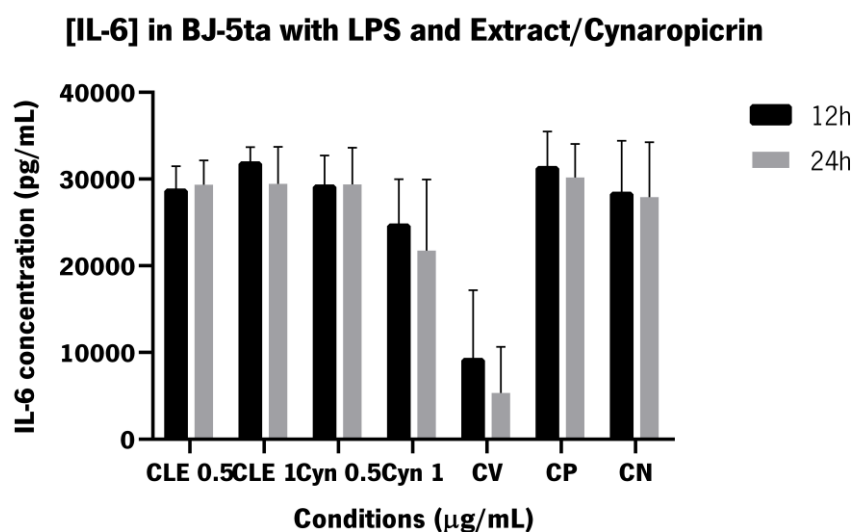
[IL-6] in BJ-5ta with LPS and Extract/Cynaropicrin

Figure 15 – IL-6 concentration released by fibroblasts BJ-5ta, 12 and 24 h after exposure to LPS. Analysed through a two-way ANOVA followed by Tukey's multiple comparisons test ($p < 0.05$; sample run in triplicates ($n=3$)).

3.2. Development of fibroblasts (BJ-5ta) and keratinocytes (HaCaT) co-culture

3.2.1. Evaluating the ideal concentration of Hoechst dye for cell staining

Concerning the development of BJ-5ta fibroblasts and HaCaT keratinocytes cell co-culture, it was imperative to create a method in which both cell types could be discerned from each other when cultured together to differentiate effects in a specific cell line. This led to the search for markers that would bind to live cells and have little to no toxicity for several days after incubation with it. Furthermore, the testing of the extracts and other assays in the co-culture would also rely on the duration of time in which the cells remained stained and their cell viability was not affected negatively by the marker.

The tested marker was a fluorescent dye named Hoechst. In the literature, the Hoechst dye is commonly used to stain live cells, due to its low toxicity in most cell types and its higher cell membrane permeation. This capability allows it to pass through the nuclei membrane and bind to rich adenine-thymine regions of the DNA. Images of Hoechst-stained cells display a blue fluorescence on the nuclei when excited by UV light (Chazotte, 2011; Zhang & Kiechle, 1997). For this assay, concentrations of 1 μg/mL and 2.5 μg/mL were used to test the optimal concentration at which the cells would sustain their fluorescence over time without the loss of cell viability. These concentrations were chosen based on

instructions and protocols for this dye (*Biotium* and *Invitrogen*).

Table 5 and **table 6** show the results of the Hoechst dye staining in BJ-5ta and HaCaT cells respectively. The pictures were taken immediately and 24, 48, and 72 h following incubation with the dye. It is clear that, for both cell lines and concentrations of the dye, the staining remained for the duration of 72 h post-incubation. However, for both concentrations of Hoechst in HaCaT cells, 48 and 72 h post-incubation, the dye began to disperse outside of the cells, a process known as leakage. Furthermore, when comparing the confluence of cells between concentrations, there was not a significant decrease in cell proliferation in either line. Due to these results, the theoretical value of concentration chosen to stain the cells on the next assays and have clear fluorescent pictures of the results was 2.5 µg/mL.

After this evaluation, another experiment was performed to assess if the timing of incubation with the dye, at a concentration of 2.5 µg/mL, had any influence on the proliferation, adherence, and viability of the cells. The results from this test would help us identify the cells that were least impacted by the dye and the optimum strategy to follow when incubating cells with it.

Figure 16 displays the cell viability of BJ-5ta and HaCaT cell lines, by MTT assay, following incubation with Hoechst dye, before (represented as pre-adherence) and after (post-adherence) the cells were seeded onto the plate. The results were normalized relative to the life control (cells without Hoechst), which was considered as 100% of viability and represented by the line Y=100 in the graph. Absorbance values greater than the life control (>100%) indicate an increase in cell proliferation, while lower values suggest the inhibition of proliferation or cellular death. HaCaT cells seemed to be more resistant to the toxicity of the Hoechst dye. It is also shown a significant difference between pre- and post-adherence for both cell lines. This difference is further proven by **table 7**, where it is clearly shown, through fluorescent pictures, the higher confluency of both cell lines if incubated with the Hoechst dye after being seeded. These results were expected and demonstrated that the best way to stain the cells with the Hoechst dye was after they were plated in the microplate.

Nevertheless, as the planned co-culture model has a layer of fibroblasts below a layer of keratinocytes, only the BJ-5ta cells were chosen to be stained with the Hoechst dye, using the method described above, in the subsequent co-culture assays. In order to distinguish between the two cell lines in the co-culture, another dye was necessary to stain HaCaT cells.

Table 5 – Hoechst staining of fibroblasts BJ-5ta, at a concentration of 1 and 2.5 µg/mL. The pictures were taken immediately and 24, 48 and 72 h following incubation with the dye. Records obtained through an inverted fluorescent microscope, after the merge of the brightfield and DAPI fluorescent images on the respective software. All the images are at a 100x magnification.
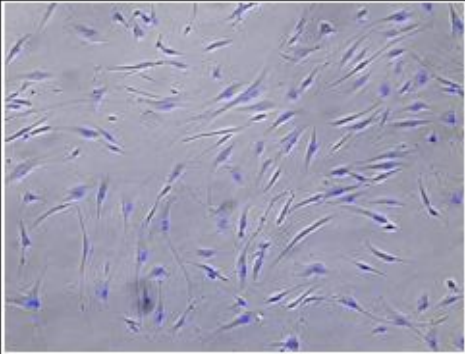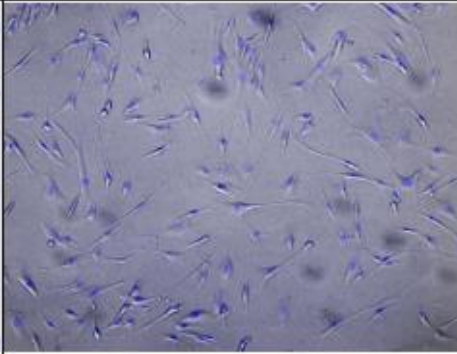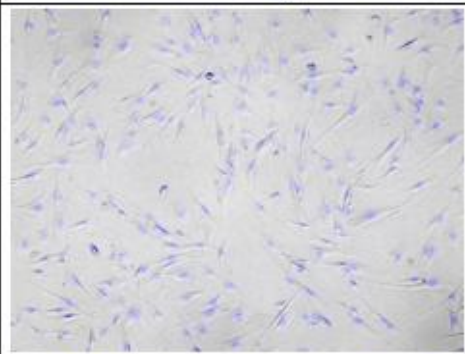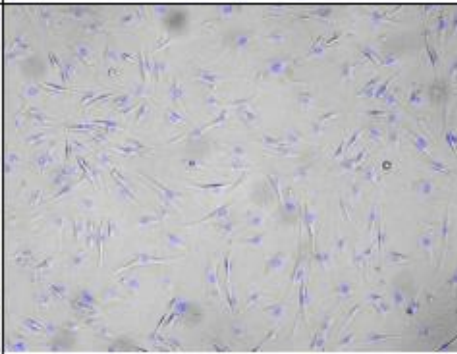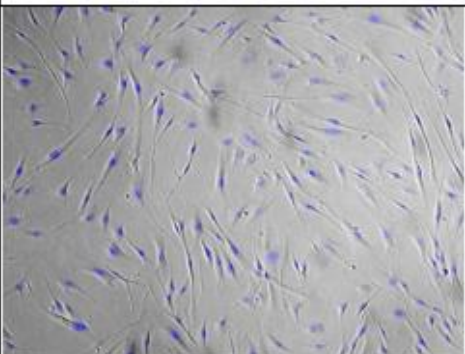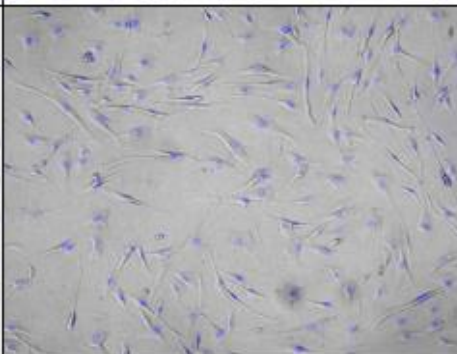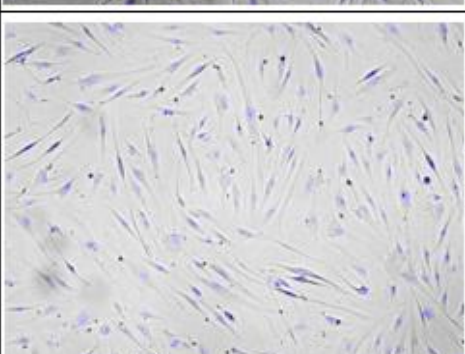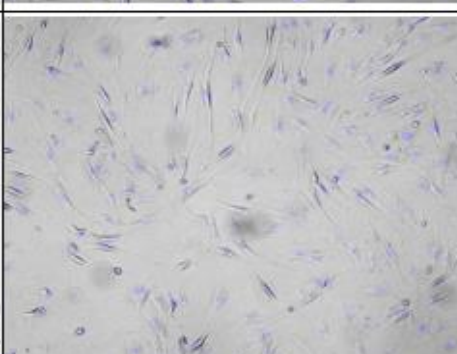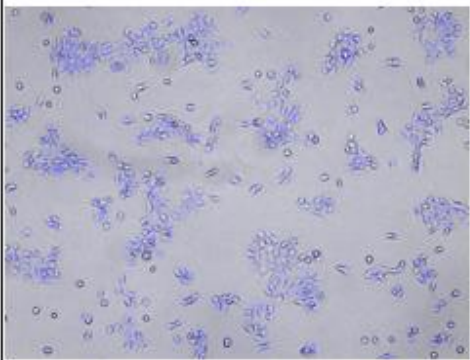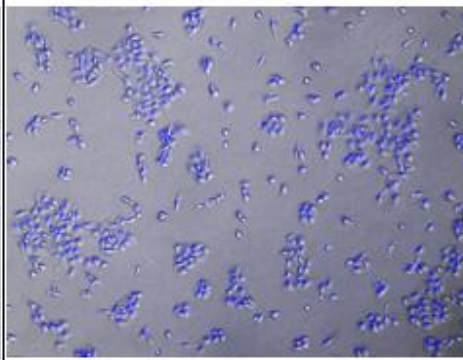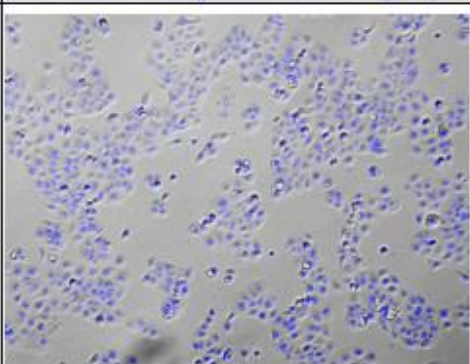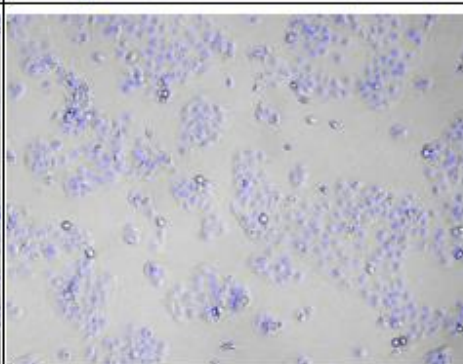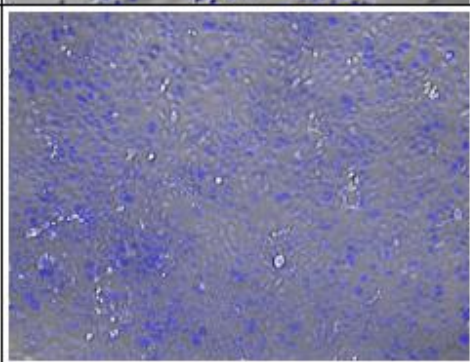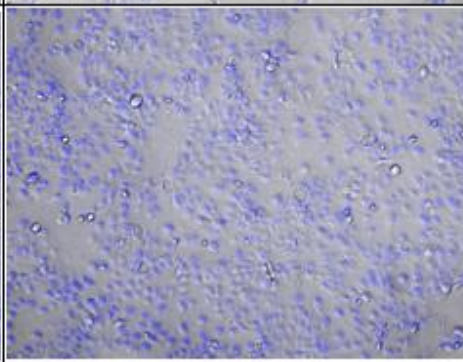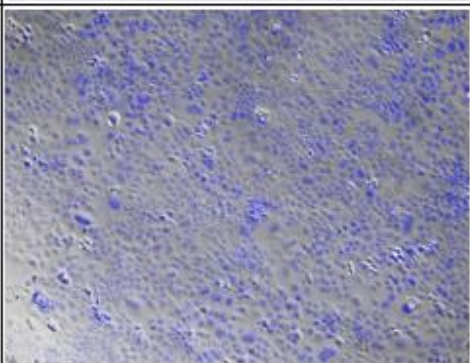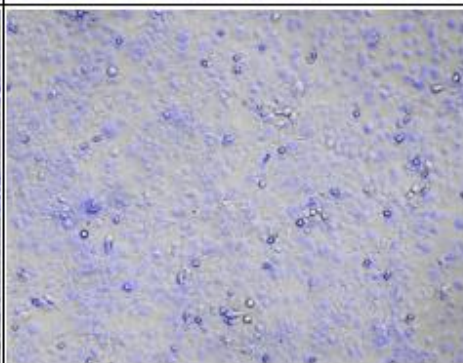
Table 6 – Hoechst staining of keratinocytes HaCaT, at a concentration of 1 and 2.5 µg/mL. The pictures were taken immediately and 24, 48 and 72 h following incubation with the dye. Records obtained through an inverted fluorescent microscope, after the merge of the brightfield and DAPI fluorescent images on the respective software. All the images are at a 100x magnification.

MTT assay - Hoechst staining in BJ-5ta and HaCaT
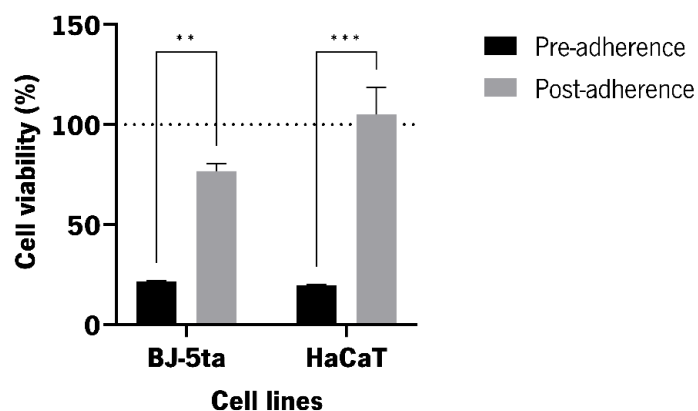
Figure 16 – Cell viability of fibroblasts BJ-5ta and keratinocytes HaCaT by MTT assay following incubation with Hoechst dye (2.5 µg/mL) before and after the cells were seeded to the plate. The viability assay was performed on the last day of the protocol. Analysed through a two-way ANOVA followed by Šidák's multiple comparisons test ($p < 0.05$; sample run in triplicates (n=3)).

Table 7 – Hoechst staining of fibroblasts BJ-5ta and keratinocytes HaCaT, incubated with the dye (2.5 µg/mL) before and after being seeded in the microplate. The pictures were taken 72 h following incubation with the dye. Records obtained through an inverted fluorescent microscope, after the merge of the brightfield and DAPI fluorescent images. All the images are at a 100x magnification, scale bar 200 µm.

Incubation with Hoechst
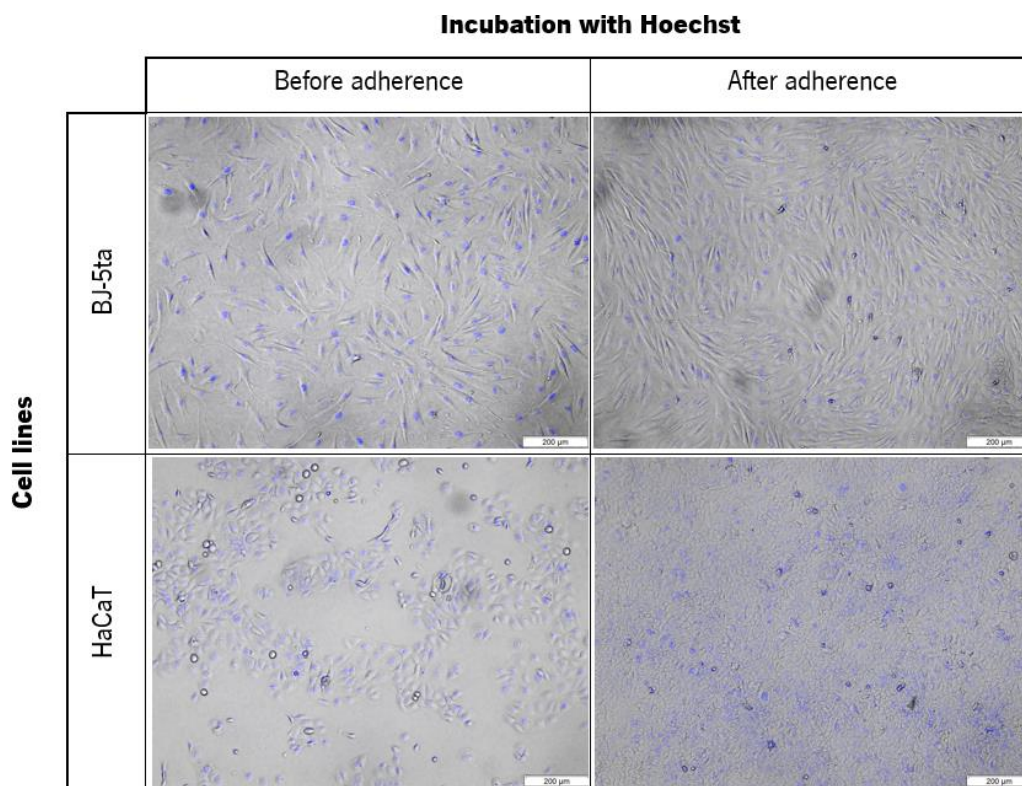
3.2.2. Determining the ideal concentration of Neutral Red dye for cell staining

Neutral red is a eurhodin dye that stains lysosomes in viable cells, being used in cytotoxicity assays to detect cell viability or drug cytotoxicity (Ates *et al.*, 2017). Viable cells can take up neutral red via active transport and incorporate the dye into their lysosomes but nonviable cells cannot take up this chromophore. Consequently, after washing, viable cells can release the incorporated dye under acidified-extracted conditions. The amount of released dye can be used to determine the total number of viable cells or drug cytotoxicity. The neutral red uptake assay provides a quantitative measurement of the number of viable cells and can be measured at OD 540 nm (Ates *et al.*, 2017; Repetto *et al.*, 2008).

To determine if the Neutral red dye was a viable option to stain HaCaT cells in the co-culture model, HaCaT keratinocytes were incubated with this compound at a concentration of 15 and 30 µg/mL. These theoretical values for concentrations were smaller than those reported in the literature (Repetto *et al.*, 2008), to verify if the cells would remain stained and viable for several days after incubation with the dye. **Table 8** shows the resultant brightfield microscopy pictures of HaCaT cells, taken 24 and 48 h after incubation with the Neutral Red marker. At a concentration of 15 µg/mL, the cells depicted low confluency, and, at the two concentrations, there was leakage of the dye to the extracellular medium. Furthermore, the fluorescence of the cells was not detected.

These results led us to rule out the use of this dye to stain HaCaT cells in co-culture. For future assays, other concentrations of the marker should be tested, and viability assays could be executed for better quantitative analysis and characterization of the impact of this dye on BJ-5ta and HaCaT cell lines. Another option is the search for alternative and better markers, particularly those that have been shown to work with the HaCaT cell line in the literature.

Table 8 – Neutral Red staining of keratinocytes HaCaT, at a concentration of 15 and 30 µg/mL.
The pictures were taken 24 and 48 h following incubation with the dye. Life control depicts the cells without staining. Brightfield pictures obtained through an inverted fluorescent microscope at a 100x magnification, scale bar 200 µm.
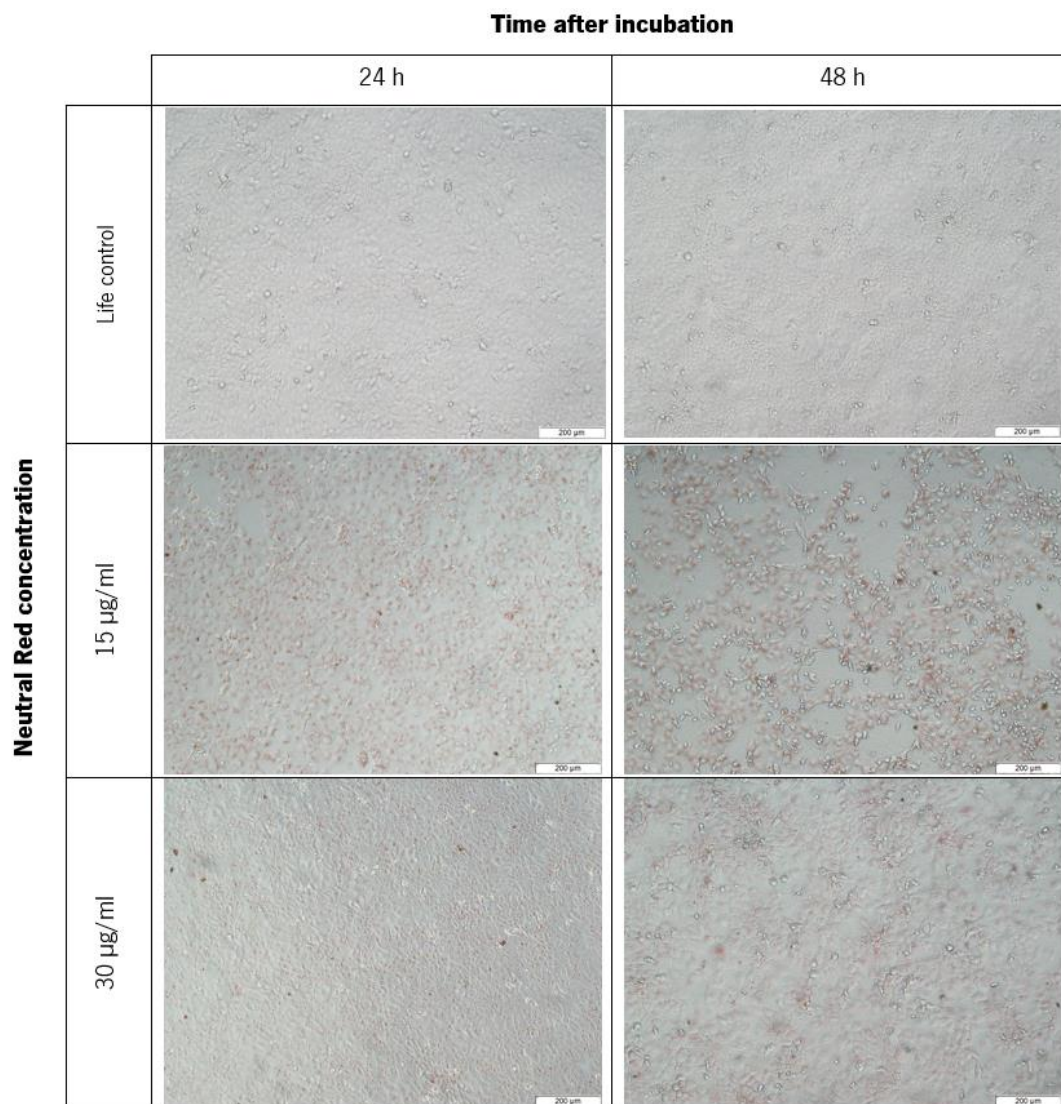
3.2.3. Hoechst staining on three different proportions of co-culture models

Although it was not possible to stain both cell lines with different dyes, due to the lack of adequate HaCat cell staining, a Hoechst staining assay of BJ-5ta cells with different ratios of unstained HaCaT cells was performed. The purpose of this work was to evaluate the disposition and behavior of both cell lines in a co-culture setting; the possibility of distinguishing the cell lines from each other by staining just one cellular type; and analyze the potential for Hoechst leakage to the extracellular space and the HaCaT

cells.

Table 9 shows the results of the Hoechst dye staining in BJ-5ta cells (2.5 μg/mL) on a co-culture setting with different proportions of HaCaT keratinocytes. These different co-culture proportions between BJ-5ta and HaCaT cells were based on the work of Sato *et al*. (1997). The pictures were taken 24 and 48 h following incubation with the dye. For the ratios of 1:2 and 1:3 (between BJ-5ta and HaCaT cells respectively), there was a clear development of a web of fibroblasts surrounding keratinocytes. This difference in morphology was expected since this is how the cells were reported to behave in literature. However, the Hoechst staining of the BJ-5ta cells didn't permit the appropriate distinction between the two cell types in co-culture. The fluorescence of the BJ-5ta cells also seemed to permeate to the unstained HaCaT cells. This may be caused by the cells' excessive confluence or possible dye leaking.

Table 9 – Co-culture of BJ-5ta and HaCaT cell lines in different proportions (1:1, 1:2 and 1:3, respectively), in which the fibroblasts BJ-5ta were stained with the Hoechst dye (2.5 μg/mL). The pictures were taken 24 and 48 h following incubation with the dye. Records obtained through an inverted fluorescent microscope, after the merge of the brightfield and DAPI fluorescent images on the respective software. All the images are at a 100x magnification, scale bar 200 μm.
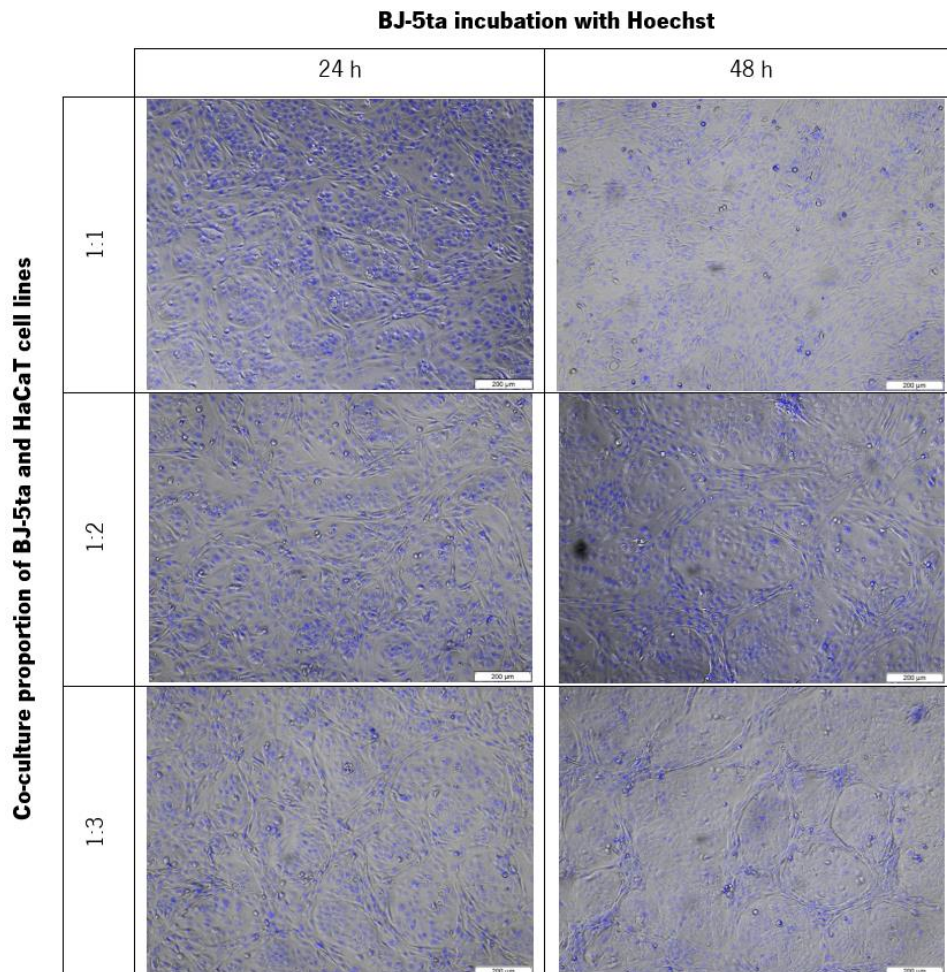
3.2.4. Study of LPS-mediated inflammation in co-culture skin model

While an appropriate cell staining protocol was not achieved, the study of the inflammatory response to LPS was conducted with the model of the co-culture in three proportions of BJ-5ta and HaCaT cells. To evaluate the effects on cell viability, toxicity, and inflammatory potential on the various models of co-culture, an MTT viability assay was performed, followed by ELISA quantification of IL-6 and IL-18. The results would allow for a better understanding of the major cell line involved in the release of the pro-inflammatory cytokines and also show the degree of inflammation that should be lowered in the following assays with the potential anti-inflammatory effect of the CLE and Cyn.

Figure 17 presents the cell viability results of the co-culture models and monoculture of each cell after being exposed to LPS. All the results were normalized relative to the life control, which was considered as 100% of viability and represented by the line Y=100 in the graph. Absorbance values greater than the life control (>100%) indicate an increase in cell proliferation, while lower values suggest the inhibition of proliferation or cellular death. Although it was anticipated that LPS could have a major impact on the viability of the cells, the graph reveals that the selected concentration did not statistically affect the cells. Recovery from the LPS incubation between the period of 24 and 48 h is perceptible in all conditions. Another noticeable result is the large decrease in viability on the 1:1 proportion of BJ-5ta and HaCaT cells, 24 h hours after LPS exposure. This could be explained by the protective role keratinocytes have in the skin (Piipponen *et al.*, 2020). In the co-culture models, this protection might be enhanced by the presence of more keratinocytes.

Figure 18 shows the quantity of IL-6 released by the cells in co-culture and monoculture, 24 h after being incubated with LPS. Expression of this inflammatory mediator is more elevated in the 1:1 co-culture, which correlates with the reduced cell viability shown in the aforementioned MTT assay. Additionally, it should be highlighted that the HaCaT cell monoculture hasn't released IL-6. This was expected since this cytokine is primarily secreted during an inflammatory reaction by fibroblasts and macrophages (Gallucci *et al.*, 2004; Johnson *et al.*, 2020).

Levels of pro-inflammatory IL-18 cytokine were also tested. A growing number of research have increased the understanding of how IL-18 mediates inflammation. Although in some illness models, IL-18 is protective, a function for IL-18 has been suggested in several autoimmune diseases, including psoriasis, macrophage activation syndrome, and sepsis. Interferon-γ is mostly produced by T-cells and natural killer cells as a result of IL-18 (Dinarello *et al.*, 2013). Keratinocytes are known to be the major producers of IL-18, constitutively expressing this pro-inflammatory cytokine at the mRNA as well as at the

protein level (Naik *et al.*, 1999). **Figure 19** depicts the values from the concentration of IL-18 in the co-culture models and monoculture, 24 h after incubation with LPS. As expected, the HaCaT cell line released greater amounts of the cytokine than the BJ-5ta cells. However, even though keratinocyte concentration rises with each proportion, IL-18 secretion decreases when compared to the control without the addition of LPS.

More research should be done to determine if these variations are due to different keratinocyte numbers by introducing controls of different concentrations of HaCaT cells monoculture, with and without LPS.

Figure 17 – Cell viability of co-culture of BJ-5ta and HaCaT cell lines in different proportions (1:1, 1:2, and 1:3, respectively) and monoculture, following inflammatory stimuli with LPS. The viability assay was performed on the last day of the protocol. Analyzed through a two-way ANOVA followed by Šidák's multiple comparisons test ($p < 0.05$; sample run in triplicates (n=3)).

IL-6 quantification in Co-culture with LPS

Figure 18 – IL-6 concentration of co-culture of BJ-5ta and HaCaT cell lines in different proportions (1:1, 1:2, and 1:3, respectively) and monoculture, following inflammatory stimuli with LPS. The control without the addition of LPS is also represented.

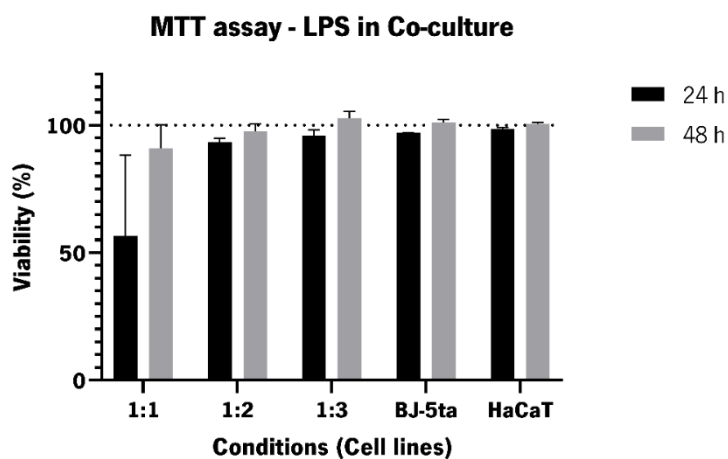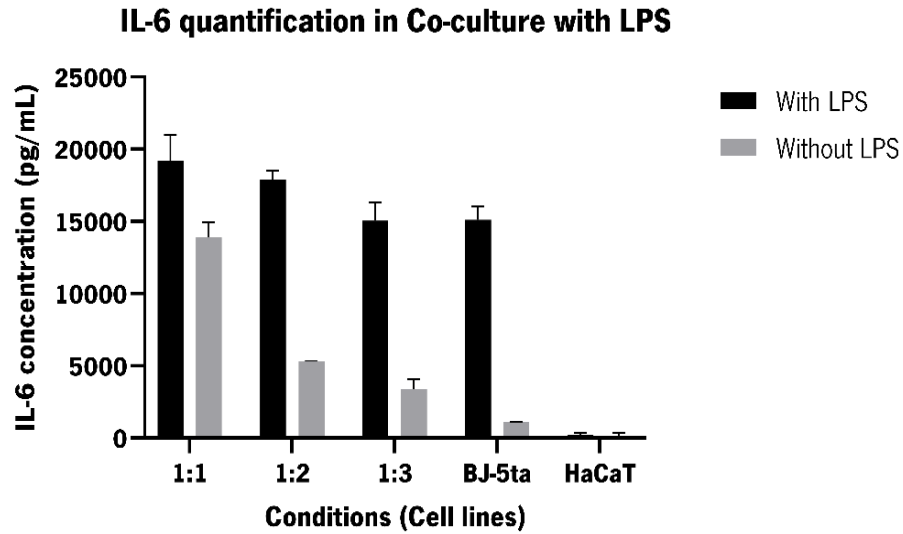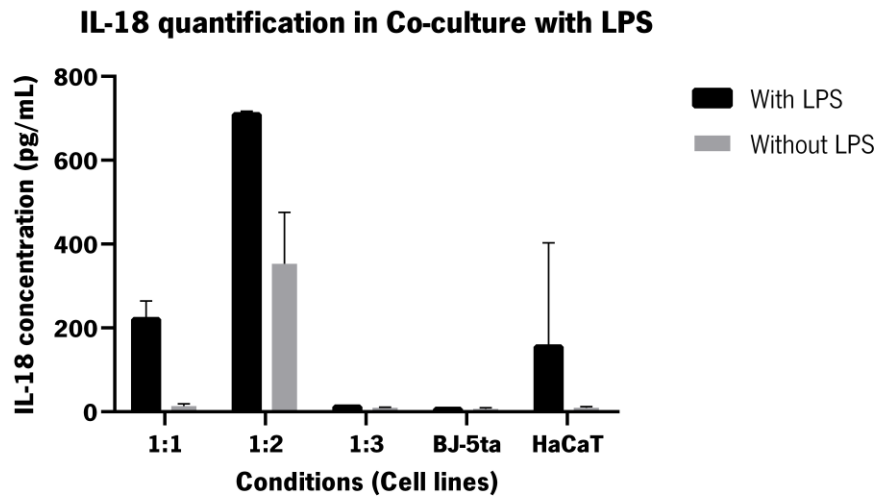## IL-18 quantification in Co-culture with LPS

Figure 19 – IL-18 concentration of the co-culture of BJ-5ta and HaCaT cell lines in different proportions (1:1, 1:2, and 1:3, respectively) and monoculture, following inflammatory stimuli with LPS. The control without the addition of LPS is also represented.

3.2.5. Evaluating the anti-inflammatory potential of CLE and cynaropicrin

To evaluate the anti-inflammatory activity of CLE and pure Cyn, the three proportions of BJ-5ta and HaCaT cell co-culture were tested. The cells were inflamed with LPS for 12 h and then incubated with CLE and Cyn for a period of 12 and 24 h. Cells incubated only with LPS were used as control of inflammation, represented as CP (positive control); and cells without the addition of any compounds, besides culture medium, were used as a negative control of inflammation. The concentrations of 0.5 and 1 µg/mL for both CLE and Cyn were chosen, reflecting the values in which cell viability was not affected, while the concentration of 5 µg/mL was tested to see the inflammatory response and subsequent effect of the extracts in a stressed cellular environment.

Figure 20 shows the quantity of IL-6 released by the inflamed cells in co-culture and monoculture, 12 and 24 h after being incubated with the CLE and Cyn. BJ-5ta and HaCaT cells in a 1:1 ratio were the ones that release most of the pro-inflammatory cytokine IL-6 under almost all conditions. As the positive control has lower values than the respective proportion of co-culture, that indicates a pro-inflammatory activity of the extract and Cyn, and specific interactions between cells are being made. It is noted that the percentage of HaCaT cells influences the degree of inflammation and the way the extract or Cyn would interact with the co-culture. In all conditions, a bigger quantity of HaCaT cells in relation to BJ-5ta lowers the inflammatory effect of the LPS.

Figure 21 illustrates the percentage of IL-18 concentration on the different proportions of co-culture following inflammatory stimuli with LPS and exposure to CLE and Cyn. Values greater than the life control indicate an increase in a pro-inflammatory response through the release of IL-18, while lower values suggest anti-inflammatory activity. At the 12 h incubation period with both CLE and Cyn, it is revealed an anti-inflammatory response to all the concentrations of extract and Cyn. In the same period, the differences in IL-18 percentages in the three co-cultures with CLE at a concentration of 0.5 µg/mL are more significant. The 1:1 ratio is often where the LPS has the greatest inflammatory effect (when compared to the life control, CV), and this result is consistent with what was observed in earlier assays. Regarding the period of 24 h, there's a big discrepancy when it is compared to the 12 h. At concentrations of 0.5 and 1 µg/mL, there's still anti-inflammatory activity by the CLE and pure Cyn. However, at a dose of 5 µg/mL of CLE and Cyn, the cells exhibit severe inflammation as seen by the vastly increased levels of IL-18 produced in comparison to the positive control (CP), especially in the 1:3 proportion. This may be due to the toxic effect of CLE and, especially, Cyn, displays at this concentration, allied to the fact that such a high confluence of cells starts to exhibit natural inflammation, as can be seen in the life controls

in this time frame.

To evaluate and distinguish each compound's effect on these models in subsequent assays, an analysis (MTT and ELISA) of the various ratios of BJ-5ta and HaCaT cells cultured with just CLE and Cyn should be performed.
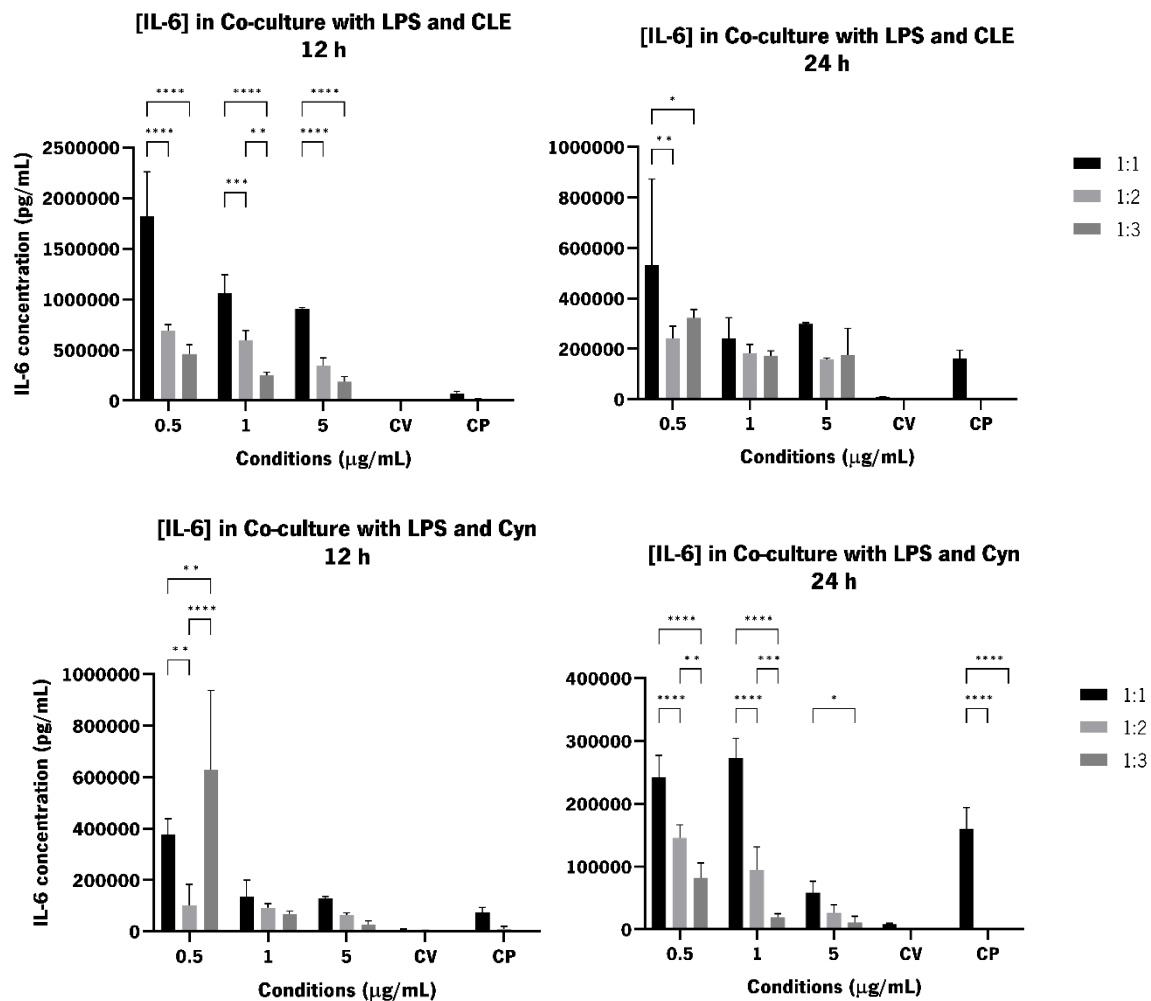
Figure 20 – IL-6 concentration of co-culture of BJ-5ta and HaCaT cell lines in different proportions (1:1, 1:2, and 1:3, respectively), following inflammatory stimuli with LPS and exposed to CLE and Cyn. CV represents the life control, with only cell medium; while CP depicts the positive control, where the cells were exposed to LPS without the extract or Cyn. Analyzed through a two-way ANOVA followed by Tukey's multiple comparisons test ($p < 0.05$; sample run in triplicates (n=3)).
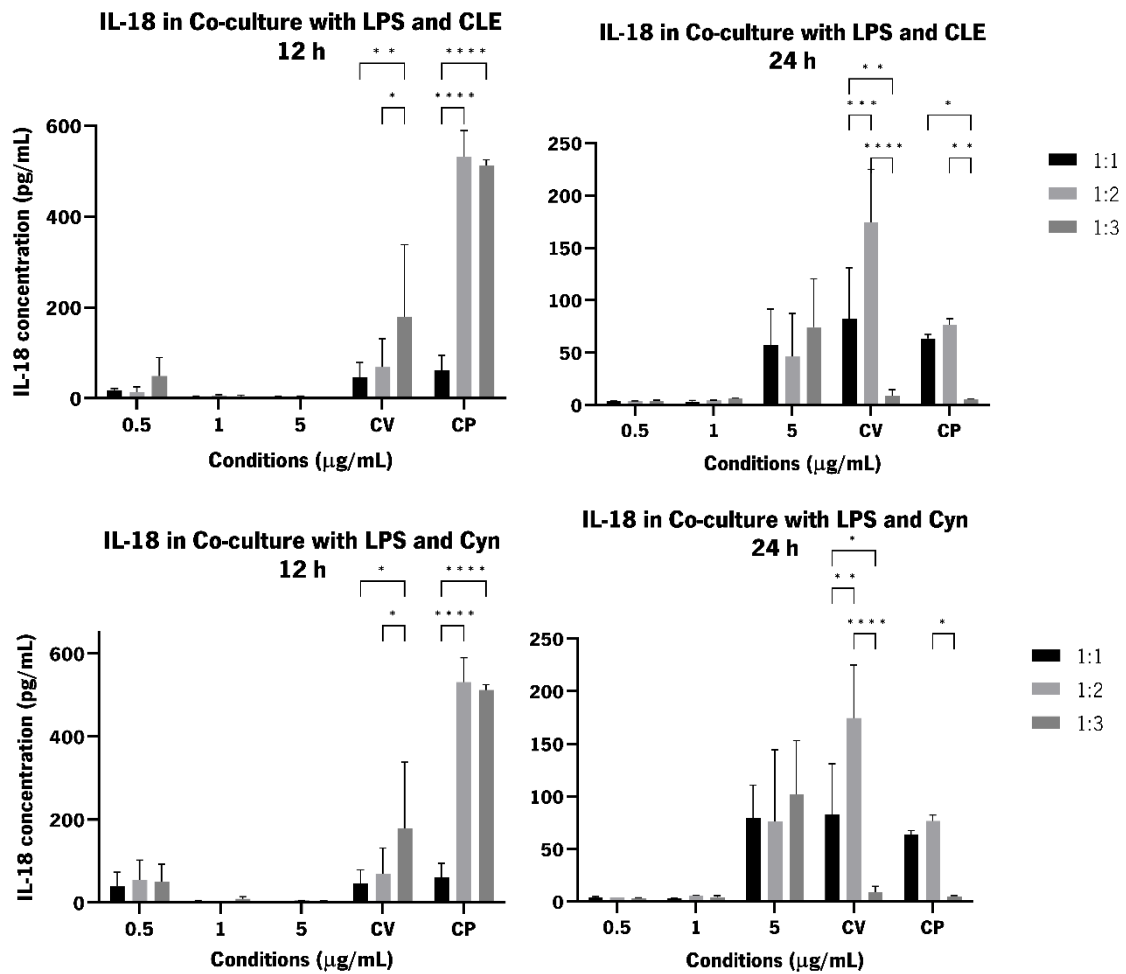
Figure 21 – IL-18 concentration of co-culture of BJ-5ta and HaCaT cell lines in different proportions (1:1, 1:2, and 1:3, respectively), following inflammatory stimuli with LPS and exposed to CLE and Cyn. CV represents the life control, with only cell medium; while CP depicts the positive control, where the cells were exposed to LPS without the extract or Cyn. Analyzed through a two-way ANOVA followed by Tukey's multiple comparisons test (p < 0.05; sample run in triplicates (n=3)).

CHAPTER 4

Conclusion and Future Perspectives

4. Conclusion and Future Perspectives

Skin conditions have a high prevalence globally, and these types of disorders are only expected to be more common due to the increase in the world's population's average life expectancy. Psoriasis is one of the most common chronic inflammatory skin disorders. Pathogenesis of the disease is significantly influenced by the invasion of inflammatory immune cells leading to sustained inflammation, uncontrolled keratinocyte proliferation, and dysfunctional differentiation. New therapies for these types of conditions can be expensive.

Because of this, crude plant extracts can be an economically and pharmacologically better alternative. These types of compounds frequently exhibit higher *in vitro* or/and *in vivo* biological activity, when compared to the isolated constituents of pure drugs made industrially or isolated from plants. This is due to the distinct kinds of beneficial interactions between the constituents of plant extracts that have been reported via pharmacokinetic interactions or synergy. This allied with the enrichment of extracts with the desired compound through the membrane fractionation process can provide a more sustainable and inexpensive solution for the production or incorporation of plant extracts in novel therapeutics.

Cynara cardunculus has been reported in several studies to have remarkable biological activities and pharmacological properties, mainly due to its major compound, cynaropicrin. Therefore, in this work, it was tested the anti-inflammatory potential of the ethanolic extracts of *C. cardunculus* leaves obtained by PUAE and fractioned membrane separation, and pure cynaropicrin in human skin cells. The main goal was to evaluate the extract and cynaropicrin in a co-culture skin model, developed to resemble the *in vivo* environment more nearly. In the future, the extract may be used topically to treat inflammatory skin conditions like psoriasis, and a simple-to-replicate co-culture model may be established.

The cytotoxic effect of the CLE was more evident in concentrations above 1 μg/mL, and the effect of Cyn was more apparent above the concentration of 5 μg/mL, for BJ-5ta fibroblasts and HaCaT keratinocytes cultured individually. However, BJ-5ta cells displayed higher sensitivity to Cyn. Both cell lines displayed more sensitivity to cynaropicrin than to the extracts.

The optimization assays for the development of a co-culture model demonstrated that the Hoechst dye could be used to stain BJ-5ta cells at a concentration of 2.5 μg/mL after they adhered to the wells of the microplate. This proved to be the best way to get a proper visualization of the cells, and one that did not affect their proliferation, viability, and adherence. This enabled the detection of the spread of BJ-5ta cells around HaCaT cells. However, this dye alone could not confer a proper visualization of each cell

line, without the addition of another marker to stain the HaCaT cells. Despite attempts to use the Neutral Red dye, HaCaT cells could not be well stained due to leakage and loss of viability.

The exposure of the different co-culture models to LPS revealed that the proportion 1:1 (BJ-5ta:HaCat cells) may be more sensitive to LPS in terms of cell viability. LPS incubation led to the production of different levels of IL-6 and IL-18 by the three different co-cultures, in comparison with the monoculture of BJ-5ta and HaCaT cells, suggesting the interaction with different numbers of keratinocytes influences the LPS-mediated response of the fibroblasts.

The immunomodulatory effect of the extract and cynaropicrin was also studied in these models of co-culture. It was noted that a bigger quantity of HaCaT cells in relation to BJ-5ta, exposed to LPS, inhibited the release of IL-6 cytokines. Additionally, a concentration of 5 μg/mL of Cyn and CLE showed the lowest values in IL-6 concentration in this model. CLE and extract had strong anti-inflammatory activity against the release of IL-18 in all models of co-culture, 12 h after incubation with LPS.

As future perspectives, it would be interesting to test other staining options of the HaCaT cell line to better distinguish the cells in the co-culture. Furthermore, to evaluate and distinguish each compound's effect on the co-culture models, viability and immunomodulation analysis of the various ratios of BJ-5ta and HaCaT cells cultured with just CLE and Cyn (without LPS incubation) should be performed. An analysis of the crosstalk between the cells could also be analyzed, with, for example, a trans-well migration assay, to better understand the chemicals behind this communication. Additionally, it would be intriguing to screen for other cytokines that are closely related to psoriasis pathology.

CHAPTER 5

Bibliography

5. Bibliography

Albanesi, C., Madonna, S., Gisondi, P., & Girolomoni, G. (2018). The interplay between keratinocytes and immune cells in the pathogenesis of psoriasis. In *Frontiers in Immunology* (Vol. 9, Issue JUL). Frontiers Media S.A. https://doi.org/10.3389/fimmu.2018.01549

Alexander, C., & Rietschel, E. Th. (2001). Bacterial lipopolysaccharides and innate immunity. *7*(3), 167–202. https://doi.org/10.1177/09680519010070030101

Atanasov, A. G., Waltenberger, B., Pferschy-Wenzig, E. M., Linder, T., Wawrosch, C., Uhrin, P., Temml, V., Wang, L., Schwaiger, S., Heiss, E. H., Rollinger, J. M., Schuster, D., Breuss, J. M., Bochkov, V., Mihovilovic, M. D., Kopp, B., Bauer, R., Dirsch, V. M., & Stuppner, H. (2015). Discovery and resupply of pharmacologically active plant-derived natural products: A review. In *Biotechnology Advances* (Vol. 33, Issue 8, pp. 1582–1614). Elsevier Inc. https://doi.org/10.1016/j.biotechadv.2015.08.001

Ates, G., Vanhaecke, T., Rogiers, V., & Rodrigues, R. M. (2017). Assaying Cellular Viability Using the Neutral Red Uptake Assay. *Methods in Molecular Biology (Clifton, N.J.)*, *1601*, 19–26. https://doi.org/10.1007/978-1-4939-6960-9_2

Bautista-Hernández, L. A., Gómez-Olivares, J. L., Buentello-Volante, B., & Bautista-de Lucio, V. M. (2017). Fibroblasts: the unknown sentinels eliciting immune responses against microorganisms. *European Journal of Microbiology and Immunology*, *7*(3), 151–157. https://doi.org/10.1556/1886.2017.00009

Bermejo, Jacinto & Delucchi, Gustavo & Charra, Gustavo & Pochettino, María & Hurrell, Julio. (2019). "Cardos" of two worlds: Transfer and resignification of the uses of thistles from the Iberian Peninsula to Argentina. Ethnobiology and Conservation. 10.15451/ec2019-03-8.05-1-22.

Berrouet, C., Dorilas, N., Rejniak, K. A., & Tuncer, N. (2020). Comparison of drug inhibitory effects (IC50) in monolayer and spheroid cultures. *BioRxiv*, 2020.05.05.079285. https://doi.org/10.1101/2020.05.05.079285

Brás, T., Neves, L. A., Crespo, J. G., & Duarte, M. F. (2022). Advances in sesquiterpene lactones extraction. *TrAC - Trends in Analytical Chemistry*, *158*. https://doi.org/10.1016/j.trac.2022.116838

Brás, T., Rosa, D., Gonçalves, A. C., Gomes, A. C., Alves, V. D., Crespo, J. G., Duarte, M. F., & Neves, L. A. (2020). Development of bioactive films based on chitosan and Cynara

cardunculus leaves extracts for wound dressings. *International Journal of Biological Macromolecules*, *163*, 1707–1718. https://doi.org/10.1016/j.ijbiomac.2020.09.109

Burslem, F. (2023). *Herbal Supplements Global Market Report 2023*. https://www.thebusinessresearchcompany.com/report/herbal-supplements-global-market-report

Cavagnero, K. J., & Gallo, R. L. (2022). Essential immune functions of fibroblasts in innate host defense. In *Frontiers in Immunology* (Vol. 13). Frontiers Media S.A. https://doi.org/10.3389/fimmu.2022.1058862

Chazotte, B. (2011). Labeling Nuclear DNA with Hoechst 33342. *Cold Spring Harbor Protocols*. https://doi.org/10.1101/PDB.PROT5557

Croteau, R., Kutchan, T.M. and Lewis, N.G. (2000) Natural Products (Secondary Metabolites). Biochemistry and Molecular Biology of Plants, 24, 1250-1319.

Che, C. T., & Zhang, H. (2019). Plant natural products for human health. In *International Journal of Molecular Sciences* (Vol. 20, Issue 4). MDPI AG. https://doi.org/10.3390/ijms20040830

Cho, J. Y., Baik, K. U., Jung, J. H., & Park, M. H. (2000). *In vitro* anti-inflammatory effects of cynaropicrin, a sesquiterpene lactone, from Saussurea lappa. In *European Journal of Pharmacology* (Vol. 398). www.elsevier.nlrlocaterejphar

Cho, J. Y., Kim, A. R., Jung, J. H., Chun, T., Rhee, M. H., & Yoo, E. S. (2004). Cytotoxic and pro-apoptotic activities of cynaropicrin, a sesquiterpene lactone, on the viability of leukocyte cancer cell lines. *European Journal of Pharmacology*, *492*(2–3), 85–94. https://doi.org/10.1016/j.ejphar.2004.03.027

Cho, J. Y., Park, J., Yoo, E. S., Baik, K. U., Jung, J. H., Lee, J., & Park, M. H. (1998). Inhibitory effect of sesquiterpene lactones from Saussurea lappa on tumor necrosis factor-alpha production in murine macrophage-like cells. *Planta Medica*, *64*(7), 594–597. https://doi.org/10.1055/S-2006-957528

Desmet, E., Ramadhas, A., Lambert, J., & van Gele, M. (2017). *In vitro* psoriasis models with focus on reconstructed skin models as promising tools in psoriasis research. *Experimental Biology and Medicine*, *242*(11), 1158–1169. https://doi.org/10.1177/1535370217710637

Dick MK, Miao JH, Limaiem F. Histology, Fibroblast. [Updated 2022 May 8]. In: StatPearls [Internet]. Treasure Island (FL): StatPearls Publishing; 2022 Jan-. Available from: https://www.ncbi.nlm.nih.gov/books/NBK541065/

Dinarello, C. A., Novick, D., Kim, S., & Kaplanski, G. (2013). Interleukin-18 and IL-18 binding

protein. *Frontiers in Immunology*, *4*(OCT), 289. https://doi.org/10.3389/FIMMU.2013.00289/BIBTEX

Elsebai, M. F., Mocan, A., & Atanasov, A. G. (2016). Cynaropicrin: A comprehensive research review and therapeutic potential as an anti-hepatitis C virus agent. In *Frontiers in Pharmacology* (Vol. 7, Issue DEC). Frontiers Research Foundation. https://doi.org/10.3389/fphar.2016.00472

Falleh, H., Ksouri, R., Chaieb, K., Karray-Bouraoui, N., Trabelsi, N., Boulaaba, M., & Abdelly, C. (2008). Phenolic composition of Cynara cardunculus L. organs, and their biological activities. *Comptes Rendus - Biologies*, *331*(5), 372–379. https://doi.org/10.1016/j.crvi.2008.02.008

Farnsworth, N., & Soejarto, D. (2009). Global Importance of Medicinal Plants. In O. Akerele, V. Heywood, & H. Synge (Eds.), *Conservation of Medicinal Plants* (pp. 25–51). Cambridge University Press.

Gallucci, R. M., Sloan, D. K., Heck, J. M., Murray, A. R., & O'Dell, S. J. (2004). Interleukin 6 Indirectly Induces Keratinocyte Migration. *Journal of Investigative Dermatology*, *122*(3), 764–772. https://doi.org/10.1111/J.0022-202X.2004.22323.X

Ghantous, A., Gali-Muhtasib, H., Vuorela, H., Saliba, N. A., & Darwiche, N. (2010). What made sesquiterpene lactones reach cancer clinical trials? In *Drug Discovery Today* (Vol. 15, Issues 15–16, pp. 668–678). https://doi.org/10.1016/j.drudis.2010.06.002

Gonçalves, A. (2020). Biological activity study of Cynara cardunculus leaves extracts: *in vitro* cell assays [Master's thesis, University of Minho]. RepositórioUM. https://hdl.handle.net/1822/78202

Gominho, J., Curt, M. D., Lourenço, A., Fernández, J., & Pereira, H. (2018). Cynara cardunculus L. as a biomass and multi-purpose crop: A review of 30 years of research. In *Biomass and Bioenergy* (Vol. 109, pp. 257–275). Elsevier Ltd. https://doi.org/10.1016/j.biombioe.2018.01.001

Gutiérrez, Diego & Scarpa, Gustavo & Rosso, Cintia. (2020). Nuevas evidencias históricas del siglo XVIII sobre la presencia de "cardos" en Argentina y sus implicancias etnobotánicas. Boletín de la Sociedad Argentina de Botánica. 55. 295-310. 10.31055/1851.2372.v55.n2.26407.

Jean, J., & Pouliot, R. (2010). *In vivo* and *In vitro* Models of Psoriasis. In D. Eberli (Ed.), *Tissue Engineering* (Vol. 18, pp. 359–382). InTech. https://doi.org/10.5772/189

Johnson, B. Z., Stevenson, A. W., Prêle, C. M., Fear, M. W., & Wood, F. M. (2020). The Role of IL-

6 in Skin Fibrosis and Cutaneous Wound Healing. *Biomedicines*, *8*(5). https://doi.org/10.3390/BIOMEDICINES8050101

Kato-Kogoe, N., Ohyama, H., Nishimura, F., Meguro, M., Yoshizawa, S., Okada, Y., Nakasho, K., Yamanegi, K., Yamada, N., Hata, M., Higashi, T., Terada, N., & Matsushita, S. (2010). Fibroblasts stimulated via HLA-II molecules produce prostaglandin E2 and regulate cytokine production from helper T cells. *Laboratory Investigation 2010 90:12*, *90*(12), 1747–1756. https://doi.org/10.1038/labinvest.2010.128

L. Kiss, A. (2022). Inflammation in Focus: The Beginning and the End. In *Pathology and Oncology Research* (Vol. 27). Frontiers Media S.A. https://doi.org/10.3389/pore.2021.1610136

Lowes, M. A., Suárez-Fariñas, M., & Krueger, J. G. (2014). Immunology of psoriasis. In *Annual Review of Immunology* (Vol. 32, pp. 227–255). Annual Reviews Inc. https://doi.org/10.1146/annurev-immunol-032713-120225

Naik, S. M., Cannon, G., Burbach, G. J., Singh, S. R., Swerlick, R. A., Wilcox, J. N., Ansel, J. C., & Caughman, S. W. (1999). Human Keratinocytes Constitutively Express Interleukin-18 and Secrete Biologically Active Interleukin-18 After Treatment with Pro-Inflammatory Mediators and Dinitrochlorobenzene. *Journal of Investigative Dermatology*, *113*(5), 766–772. https://doi.org/10.1046/J.1523-1747.1999.00750.X

Ortiz-Lopez, L. I., Choudhary, V., & Bollag, W. B. (2022). Updated Perspectives on Keratinocytes and Psoriasis: Keratinocytes are More Than Innocent Bystanders. *Psoriasis: Targets and Therapy*, *Volume 12*, 73–87. https://doi.org/10.2147/ptt.s327310

Paço, A., Brás, T., Santos, J. O., Sampaio, P., Gomes, A. C., & Duarte, M. F. (2022). Anti-Inflammatory and Immunoregulatory Action of Sesquiterpene Lactones. In *Molecules* (Vol. 27, Issue 3). MDPI. https://doi.org/10.3390/molecules27031142

Paulie, S., Perlmann, P., & Perlmann, H. (2022). Enzyme Linked Immunosorbent Assay. *Cell Biology: A Laboratory Handbook*, 533–538. https://doi.org/10.1016/B978-012164730-8/50065-4

Piipponen, M., Li, D., & Landén, N. X. (2020). The Immune Functions of Keratinocytes in Skin Wound Healing. *International Journal of Molecular Sciences*, *21*(22), 1–26. https://doi.org/10.3390/IJMS21228790

Plikus, M. v., Wang, X., Sinha, S., Forte, E., Thompson, S. M., Herzog, E. L., Driskell, R. R., Rosenthal, N., Biernaskie, J., & Horsley, V. (2021). Fibroblasts: Origins, definitions, and functions in health and disease. In *Cell* (Vol. 184, Issue 15, pp. 3852–3872). Elsevier B.V.

https://doi.org/10.1016/j.cell.2021.06.024

Raharja, A., Mahil, S. K., & Barker, J. N. (2021). Psoriasis: A brief overview. In *Clinical Medicine, Journal of the Royal College of Physicians of London* (Vol. 21, Issue 3, pp. 170–173). Royal College of Physicians. https://doi.org/10.7861/CLINMED.2021-0257

Ramos, P. A. B., Guerra, A. R., Guerreiro, O., Freire, C. S. R., Silva, A. M. S., Duarte, M. F., & Silvestre, A. J. D. (2013). Lipophilic extracts of cynara cardunculus L. var. altilis (DC): A source of valuable bioactive terpenic compounds. *Journal of Agricultural and Food Chemistry*, *61*(35), 8420–8429. https://doi.org/10.1021/jf402253a

Ramos, P. A. B., Guerra, Â. R., Guerreiro, O., Santos, S. A. O., Oliveira, H., Freire, C. S. R., Silvestre, A. J. D., & Duarte, M. F. (2017). Antiproliferative effects of cynara cardunculus L. Var. altilis (DC) lipophilic extracts. *International Journal of Molecular Sciences*, *18*(1). https://doi.org/10.3390/ijms18010063

Rendon, A., & Schäkel, K. (2019). Psoriasis pathogenesis and treatment. In *International Journal of Molecular Sciences* (Vol. 20, Issue 6). MDPI AG. https://doi.org/10.3390/ijms20061475

Repetto, G., del Peso, A., & Zurita, J. L. (2008). Neutral red uptake assay for the estimation of cell viability/cytotoxicity. *Nature Protocols*, *3*(7), 1125–1131. https://doi.org/10.1038/NPROT.2008.75

Riss, T. L., Moravec, R. A., Niles, A. L., Duellman, S., Benink, H. A., Worzella, T. J., & Minor, L. (2016). Cell Viability Assays. In *Assay Guidance Manual* (pp. 353–378). Eli Lilly & Company and the National Center for Advancing Translational Sciences. https://www.ncbi.nlm.nih.gov/books/NBK144065/

Russell, F. D., Visagie, J. C., & Noll, J. L. (2022). Secretion of IL-6 by fibroblasts exposed to Australian honeys involves lipopolysaccharide and is independent of floral source. *Scientific Reports 2022 12:1*, *12*(1), 1–10. https://doi.org/10.1038/s41598-022-21130-6

Saggini, A., Chimenti, S., & Chiricozzi, A. (2014). IL-6 as a druggable target in psoriasis: Focus on pustular variants. *Journal of Immunology Research*, *2014*. https://doi.org/10.1155/2014/964069

Sandberg, F., & Corrigan, D. (2001). *Natural Remedies: Their Origins and Uses* (1st ed.). Taylor & Francis.

Saranraj, P., Sivasakthi, S., & Deepa, M. S. (2016). Phytochemistry of pharmacologically important medicinal plants – A Review. *International Journal of Current Research in Chemistry and Pharmaceutical Sciences*, *3*(11), 56–66.

https://doi.org/10.22192/ijcrcps.2016.03.11.009

Sato, T., Kirimura, Y., & Mori, Y. (1997). The co-culture of dermal fibroblasts with human epidermal keratinocytes induces increased prostaglandin E2 production and cyclooxygenase 2 activity in fibroblasts. *The Journal of Investigative Dermatology*, *109*(3), 334–339. https://doi.org/10.1111/1523-1747.EP12335935

Siegel, RL, Miller, KD, Fuchs, HE, Jemal, A. Cancer statistics, 2022. CA Cancer J Clin. 2022. https://doi.org/10.3322/caac.21708

Stockert, J. C., Horobin, R. W., Colombo, L. L., & Blázquez-Castro, A. (2018). Tetrazolium salts and formazan products in Cell Biology: Viability assessment, fluorescence imaging, and labeling perspectives. *Acta Histochemica*, *120*(3), 159–167. https://doi.org/10.1016/J.ACTHIS.2018.02.005

Szymański, Ł., Jęderka, K., Cios, A., Ciepelak, M., Lewicka, A., Stankiewicz, W., & Lewicki, S. (2020). A simple method for the production of human skin equivalent in 3D, multi-cell culture. *International Journal of Molecular Sciences*, *21*(13), 1–11. https://doi.org/10.3390/ijms21134644

Vaou, N., Stavropoulou, E., Voidarou, C., Tsakris, Z., Rozos, G., Tsigalou, C., & Bezirtzoglou, E. (2022). Interactions between Medical Plant-Derived Bioactive Compounds: Focus on Antimicrobial Combination Effects. *Antibiotics*, *11*(8). https://doi.org/10.3390/antibiotics11081014

Veeresham, C. (2012). Natural products derived from plants as a source of drugs. In *Journal of Advanced Pharmaceutical Technology and Research* (Vol. 3, Issue 4, pp. 200–201). Wolters Kluwer Medknow Publications. https://doi.org/10.4103/2231-4040.104709

Wang, J. N., & Li, M. (2020). The Immune Function of Keratinocytes in Anti-Pathogen Infection in the Skin. In *International Journal of Dermatology and Venereology* (Vol. 3, Issue 4, pp. 231–238). Wolters Kluwer Health. https://doi.org/10.1097/JD9.0000000000000094

Zhang, X., & Kiechle, F. L. (1997). Hoechst 33342-induced Apoptosis in BC3H-1 Myocytes. *Annals Of Clinical And Laboratory Science*, *27*(4), 260–275.